AFTAC Project No. VT/1705





# EXTENDED ARRAY EVALUATION PROGRAM

Quarterly Report No. 2

1 July 1971 to 30 September 1971

T. W. Harley, Program Manager
Area Code 703, 836-3882 Ext-300

TEXAS INSTRUMENTS INCORPORATED
Services Group
P.O. Box 5621
Dallas, Texas 75222

Contract No. F33657-71-C-0843
Amount of Contract: $511,580
Beginning 1 April 1971
Ending 31 March 1972



Prepared for

AIR FORCE TECHNICAL APPLICATIONS CENTER
Washington, D.C. 20333

Sponsored by

ADVANCED RESEARCH PROJECTS AGENCY
Nuclear Monitoring Research Office
ARPA Order No. 1714
ARPA Program Code No. 1F10

15 October 1971



Acknowledgement: This research was supported by the Advanced Research Projects Agency, Nuclear Monitoring Research Office, under Project VELA-UNIFORM, and accomplished under the technical direction of the Air Force Technical Applications Center under Contract No. F33657-71-C-0843.

This document is subject to special export controls and each transmittal to foreign governments or foreign nationals may be made only with prior approval of Chief, AFTAC.

Qualified users may request copies of this document from:

Defense Documentation Center
Cameron Station
Alexandria, Virginia 22314

AFTAC Project No. VT/1705





# EXTENDED ARRAY EVALUATION PROGRAM

Quarterly Report No. 2

1 July 1971 to 30 September 1971

T. W. Harley, Program Manager
Area Code 703, 836-3882 Ext-300

TEXAS INSTRUMENTS INCORPORATED
Services Group
P.O. Box 5621
Dallas, Texas 75222

Contract No. F33657-71-C-0843
Amount of Contract: $511,580
Beginning 1 April 1971
Ending 31 March 1972

Prepared for

AIR FORCE TECHNICAL APPLICATIONS CENTER
Washington, D.C. 20333

Sponsored by

ADVANCED RESEARCH PROJECTS AGENCY
Nuclear Monitoring Research Office
ARPA Order No. 1714
ARPA Program Code No. 1F10

15 October 1971



Acknowledgement: This research was supported by the Advanced Research Projects Agency, Nuclear Monitoring Research Office, under Project VELA-UNIFORM, and accomplished under the technical direction of the Air Force Technical Applications Center under Contract No. F33657-71-C-0843.

This document is subject to special export controls and each transmittal to foreign governments or foreign nationals may be made only with prior approval of Chief, AFTAC.

Qualified users may request copies of this document from:

Defense Documentation Center
Cameron Station
Alexandria, Virginia 22314

UNCLASSIFIED
Security Classification

## DOCUMENT CONTROL DATA - R & D

*(Security classification of title, body of abstract and indexing annotation must be entered when the overall report is classified)*

1. ORIGINATING ACTIVITY *(Corporate author)*
Texas Instruments Incorporated
Services Group
P.O. Box 5621, Dallas, Texas 75222

2a. REPORT SECURITY CLASSIFICATION
UNCLASSIFIED

2b. GROUP

3. REPORT TITLE
Extended Array Evaluation Program, Quarterly Report No. 2

4. DESCRIPTIVE NOTES *(Type of report and inclusive dates)*
Second Quarterly Report, 1 July 1971 to 30 September 1971

5. AUTHOR(S) *(First name, middle initial, last name)*
Harley, Terence W.

| 6. REPORT DATE | 7a. TOTAL NO. OF PAGES | 7b. NO. OF REFS |
|---|---|---|
| 15 October 1971 | 102 | 5 |

| 8a. CONTRACT OR GRANT NO. | 9a. ORIGINATOR'S REPORT NUMBER(S) |
|---|---|
| Contract No. F33657-71-C-0843 | |
| b. PROJECT NO. | |
| c. AFTAC Project No. VT/1705 | 9b. OTHER REPORT NO(S) *(Any other numbers that may be assigned this report)* |
| d. | |

10. DISTRIBUTION STATEMENT
APPROVED FOR PUBLIC RELEASE; DISTRIBUTION UNLIMITED.
with prior approval of Chief, AFTAC

| 11. SUPPLEMENTARY NOTES | 12. SPONSORING MILITARY ACTIVITY |
|---|---|
| ARPA Order No. 1714 | Advanced Research Projects Agency<br>Nuclear Monitoring Research Office<br>Arlington, VA |

13. ABSTRACT

This second quarterly report discusses work performed under the Extended Evaluation of ALPA, NORSAR, and LPE Data program, Contract F33657-71-C-0843. Work to date in the following areas is discussed:

- Software upgrades
- ALPA evaluation
- NORSAR long period evaluation
- NORSAR short period evaluation
- LPE evaluation

DD FORM 1 NOV 65 1473

UNCLASSIFIED
Security Classification

| 14. KEY WORDS | LINK A | | LINK B | | LINK C | |
|---|---|---|---|---|---|---|
| | ROLE | WT | ROLE | WT | ROLE | WT |
| Extended Evaluation of ALPA, NORSAR and LPE data<br><br>Quarterly Report No. 2, 1 July 1971 to 30 September 1971<br><br>ALPA Evaluation<br><br>NORSAR Long Period Evaluation<br><br>NORSAR Short Period Evaluation<br><br>LPE Evaluation | | | | | | |

TABLE OF CONTENTS

LIST OF TABLES

## LIST OF FIGURES

# I. INTRODUCTION AND SUMMARY

This quarterly report describes progress made during the past quarter, 1 July 1971 to 30 September 1971, on the Extended Evaluation of ALPA, NORSAR and LPE Data program being conducted by Texas Instruments Incorporated at the Seismic Array Analysis Center. The program consists of the following seven tasks:

- Continued evaluation of the Alaskan Long Period Array (ALPA)
- Evaluation of the long period Norwegian Seismic Array (NORSAR)
- Evaluation of the short period Norwegian Seismic Array
- Evaluation of the stations of the Long Period Experiment (LPE) network
- Investigation of network processing and analysis techniques
- Adaptive processing studies
- Investigation of high-resolution frequency-wave number spectral estimation techniques

The software required to perform the evaluation was developed under a previous contract ( Contract F33657-60-C-1063). During the past quarter some modifications were made to the software; these are discussed in Section II of this report. Detailed updates to the documentation will be submitted to VELA Seismological Center under separate cover.

Section III describes work performed during the quarter on the ALPA evaluation task. Included are a brief description of routine event processing, results of a study to separate interfering events with a beamsteer processor, a comparison of the signal degradation of off-line and on-line beamsteers, and results of an evaluation of two-component Rayleigh wave processing.

Section IV describes work performed on the NORSAR long period evaluation task. The evaluation effort during the quarter was directed toward

obtaining and processing the first suite of events and noise samples. Due to problems encountered in finding useable data, only a limited number of events and noise samples were analyzed. These problems are discussed along with the general data quality. Analysis results included are signal analysis, a discussion of the ambient noise field, some initial results from the array processing task, and first results of a chirp filter study.

Section V describes work performed under the NORSAR short period evaluation task. Work was concentrated on analysis of the general quality of the 132 channel NDPC data tapes, noise analysis, a study of the signal characteristics, and an investigation of array beamforming techniques.

Section VI discusses the work performed on the LPE task. To date the LPE evaluation was limited by the quality of the data received at SAAC. However, a limited amount of data from early 1971 have been processed and analyzed. Analysis of the noise field for this time period, and a very preliminary discussion of the detection capabiltiy of each station and the network are included. Also, the behavior of the $M_S$-$m_b$ classification parameter is described.

No new results for the adaptive processing studies are available. Also, no results from the spectral analysis task are available.

## II. SOFTWARE UPGRADES

### A. Introduction

During the past quarter a few modifications were made to the analysis software. Software changes were made to EVPLOT of the LP array evaluation package, LXMERG and LXDALL of the LPE package, and NSPED of the NORSAR SP package. This section describes the program modifications; appropriate updates to the documentation will be submitted to VSC under separate cover in the near future.

### B. Long-Period Array Evaluation Package

#### 1. EVPLOT

During the past quarter, two changes were made in EVPLOT. The event time drawn on the plot is now updated by the time interval of the skipped initial segments, if any. An amplitude conversion constant and alternative rotation subroutine call are provided to allow the program to be used for data from arrays other than ALPA.

### C. Long-Period Experiment Evaluation Package

#### 1. LXMERG

Several changes have been made in LXMERG during the past quarter on the basis of further operating experience. The intermediate tape specification card now uses the assigned tape system numbers, rather than a purely internal tape index number. A console interrupt check has been included in the main merge record processing loop to permit truncation of the merge interval while the program is running. This capability is valuable for partial recovery when serious input tape problems develop late in the merge.

Input tapes have been found to contain occasional records with spurious timing words. To permit the merge program to access correct data subsequent to such records, an additional timing test has been included: if the input record time is greater than the end of the merge interval, the record is regarded as an error condition and is ignored.

Subroutine TPROC has been coded and is now used for checking the timing codes in the input intermediate format merge records. The complex subscripting involved in this checking was not efficient in FORTRAN; the new routine is coded in ALC.

Error recovery is now attempted for all output tape error conditions. Erase-gaps and record repeats are attempted up to 50 times. On the final library tape, a maximum of 11000 output records are written on each tape, since the system apparently does not always recognize the end-of-tape reflective marker. Finally, the start and stop times of the individual output tape reels are printed to provide more convenient record keeping.

2. LXDALL

During the past quarter, minor changes were made in the output tape format to conform to revised specifications. Output error recovery coding was included: such conditions as write-parity now cause erase-gaps and output re-attempts to be generated up to fifty times. Changes were also made in the tape handling conventions to allow multiple input and output reels to be processed on the same run.

## D. NORSAR Short-Period Array Evaluation Package

### 1. NSPED

During the past quarter, initial processing of large numbers of NDPC tapes was carried out, and several program changes were made as a result. It was assumed, during program development, that the NDPC tapes would each contain data for a single time block of no more than 2.5 hours duration. In practice, each tape contains data for two or more time blocks of ususally 30 minutes each, separated by intervals of days, and not always in correct temporal order. Consequently, the tape input subroutine READND had to be modified to first rewind the tape, then search forward regardless of record timing. To avoid excessive search time, a pause and interrupt check were included in NSPED to allow the analyst to instruct the program at the beginning of each edit search whether to process the current input tape or request the next tape. Changes were also made to facilitate input error recovery: retry attempts are now made up to thirty times for such conditions as read-parity and short records.

## III. ALPA EVALUATION

### A. Introduction

Routine processing of events received at ALPA has continued during this quarter. A brief description of this work appears in part B. In addition several investigative efforts have been performed. Part C describes an attempt to separate interfering events with a beamsteer processor. In part D a comparison of the signal degradation of off-line and on-line beamsteers is discussed. Part E gives recent results of the two-component Rayleigh-wave processor evaluation. Future plans are discussed in part F.

### B. Routine Processing

Approximately fifty events which occured during the month of June have been processed. This includes beamsteering, bandpass filtering, matched filtering when necessary, and the measurement of classification parameters. Shear wave amplitudes are now included routinely in this last category. In addition to the above, seven events from known underground test sites have been processed. In none of the cases considered was the full array operational. Current processing is concentrated on the month of July. It is believed that data from the latter part of July will yield a higher percentage of usable sites.

The optimum bandpass filter for shear-wave extraction has been determined. A suite of nine events was selected on the basis of having clear arrivals in the shear-wave beamsteer. Bodywave magnitudes ranged from 4.7 to 6.7, and deltas ranged from 27 degrees to 77 degrees. In each case the component having the largest shear-wave amplitude, usually the transverse, was bandpass filtered with a suite of filters spanning the range 0.012 Hz to 0.102 Hz. The figure of merit used was the ratio of peak signal amplitude to RMS noise value in the bandpassed beam. In five of the nine cases the best performance was achieved with an 0.027 Hz to 0.059 Hz bandwidth; in three cases an 0.020 Hz

to 0.051 Hz bandwidth was best. It has been determined previously to routinely use an 0.025 Hz to 0.055 Hz bandpass filter on the surface-wave beams. In view of these results that filter also appears to be appropriate for the shear-wave beams. The degradation in signal amplitude resutling from bandpass filtering was computed for the eight cases mentioned above. The average degradation was found to be 1.7 dB.

Seven one-hour noise samples were edited to enable comparison of the ALPA and NORSAR noise levels. Figure III-1 shows the RMS values of these samples for the band 0.023 Hz to 0.051 Hz, averaged across the array. Only the vertical component for NORSAR is shown. The presence of highly site-dependent very long-period noise on the NORSAR horizontal seismometers makes an array average of questionable value. Based on this brief sample it appears that the vertical component noise levels at the two arrays are fairly similar. The vertical component noise at NORSAR in this band is largely dominated by the microseisms. Thus the high value of twelve millimicrons on day 191 is due to the presence of relatively strong microseismic activity. Note that the NORSAR value was not available for day 213.

C. Interfering Event Analysis

On 26 July, 1971 the SAAC bulletin reported four Solomon Islands events and two Sinkiang events occuring between 0100 and 0300 GMT. The Solomon bodywave magnitudes given were 6.0, 5.1, 6.5, and 6.4; the Sinkiang magnitudes were 6.1 and 5.1. It was suggested that these events be processed as an interfering event study. In an effort to separate the events temporally and directionally the data in this interval were broken into non-overlapping twelve minute and forty-eight second time gates. High-resolution wavenumber spectra were computed for each time gate at 0.039 Hz and at 0.047 Hz. The first five such gates which spanned the surface wave arrivals from the

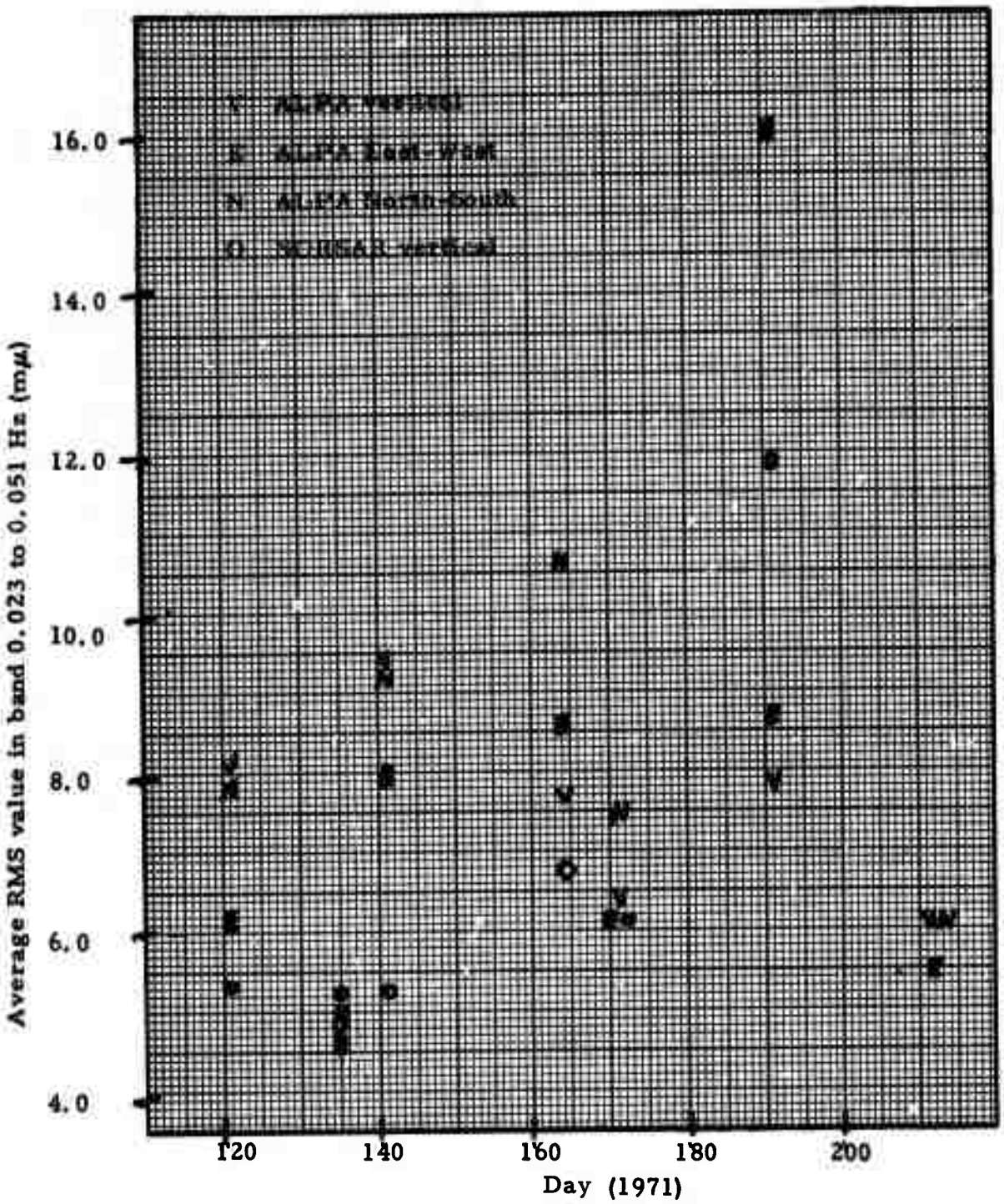


FIGURE III-1
COMPARISON OF ALPA AND NORSAR RMS NOISE LEVELS

first three Solomon events and the first Sinkiang event showed peaks only in the general direction of the Solomon events. The sixth gate included the latter portions of the fourth Solomon event, the second Sinkiang event, and an $m_b = 6.2$ Solomon event published later in the PDE bulletin. These wavenumber spectra showed a peak at 3.3 km/sec, 345 degrees, about 20° from the correct Sinkiang great circle azimuth. This peak, while quite weak, may actually represent the Sinkiang event.

Surface wave beamsteers were formed for both azimuths using 17 available sites. At this time it was determined that the first Solomon Islands event has a surface wave magnitude of 7.7. This abnormally high value was later confirmed by the PDE bulletin which reported $M_s = 7.9$. As a result all of the succeeding Solomon Islands events were obscurred by the coda of this event and could not be detected. The Sinkiang beam significantly attenuated this event but not enough to permit detection of either Sinkiang event. It is likely that the largest of the Sinkiang events was at least 1.5 surface-wave magnitude units smaller than the obscurring Solomon Islands event. As a last resort the Sinkiang beam was match filtered with a previously recorded Sinkiang master waveform. This too was unsuccessufl in uncovering either Sinkiang event. Apparently the differences in surface wave magnitudes were too great to permit extraction of the interfered Sinkiang events.

D. Comparison of On-Line and Off-Line Beams

The purpose of this study was to compare surface wave beamsteer outputs formed by the on-line processor with those formed using off-line software. Differences in the two outputs are beamsteer azimuths and site selction prior to beam formation. Beamsteer azimuths used in the off-line software correspond to the expected great circle path. In the on-line processor; however, surface wave beamsteer azimuths are preset at initialization time.

Normally, six azimuths in increments of 60° have been chosen for on-line beamsteering. Site selection for off-line beamsteers are made by the analyst using Calcomp plots of each site. The on-line beams are formed from all sites that have passed the software quality checks for a given 15 second block of data (Documentation of On-Line Software, 1971). It is therefore possible for the number of sites used in beamsteering an event with the on-line processor to vary within the duration of the event.

Data used for this study were chosen from events already processed through the off-line software and reported in the Final Report (Texas Instruments, 1971). The separation between great circle path and available on-line beamsteer azimuths for these events ranged from zero to 35 degrees. The suite included both high and low signal-to-noise ratio events. The ten events chosen are given in Table III-1. An additional five events were selected for the comparison but were not accessible by the on-line plot software.

A software program to generate Calcomp plots of on-line beams recorded by the IIRSPS system was borrowed from SAAC. However, on-line library tapes containing the desired events were generated by the Interim ALPA system. This necessitated considerable software change. Calcomp plots of the off-line beamsteers were already available for the comparison.

Signal degradation in the beamsteer output due to deviations in the beam azimuth can be anticipated by examinimg the beamsteer response in f-$\vec{k}$-space. The beam pattern for the seven element array is such that no more than 3 dB signal degradation would be expected for azimuthal variations as large as 40 degrees. Less than 1 dB degradation is espected for variations less than 20 degrees. Although no actual comparison of on-line and off-line beams for a full 19 element array is possible at this time, it should be noted that the expected signal degradation for off azimuth beams is more severe. In order to be certain that no more than 1 dB attenuation in signal occurs, an azimuth within 15° of the great circle path is required. Likewise, azimuthal variations of 35° would

TABLE III-1

ON-LINE OFF-LINE BEAMSTEER PERFORMANCE

(Attenuation in dB)

| Name | Off-Line Azimuth | On-Line Azimuth 1 | LR-V Amplitude Attenuation | LR-R Amplitude Attenuation | LQ-T Amplitude Attenuation | On-Line Azimuth 2 | LR-V Amplitude Attenuation | LR-R Amplitude Attenuation | LQ-T Amplitude Attenuation | $m_b$ | $M_s$ |
|---|---|---|---|---|---|---|---|---|---|---|---|
| KAM/179/11 | 271° | 275° | -1.0 | -0.4 | 0.0 | 235° | 0.0 | 1.5 | 0.6 | 5.8 | 4.4 |
| SIN/221/16 | 324° | 330° | 0.0 | 1.5 | * | 350° | 0.0 | 5.5 | * | 4.5 | 3.5 |
| KAM/170/18 | 275° | 275° | 0.2 | 0.0 | 1.1 | | | | | 5.2 | 3.9 |
| MON/171/08 | 311° | 315° | 0.4 | 1.4 | 4.2 | 275° | 2.0 | 10.0 | 4.2 | 4.1 | 3.7 |
| CHI/220/11 | 323° | 330° | 0.0 | 0.0 | -0.2 | 350° | 0.4 | 1.0 | 1.2 | 4.7 | 4.0 |
| KUR/220/14 | 271° | 275° | -1.4 | -1.1 | -1.6 | | | | | 4.4 | 2.9 |
| KUR/219/01 | 270° | 275° | -0.1 | 0.0 | -0.2 | | | | | 5.0 | 3.9 |
| KUR/219/13 | 270° | 275° | -4.3 | 0.0 | 0.0 | | | | | 4.5 | 3.7 |
| KUR/178/03 | 268° | 275° | 0.0 | 0.1 | 0.0 | 235° | 1.2 | 0.1 | 1.8 | 4.8 | 3.8 |
| ALB/178/18 | 10° | 355° | 0.0 | 2.0 | 0.0 | 35° | 1.7 | 4.1 | 0.0 | 4.5 | 3.4 |

* No Signal

be expected to cause at least 6 dB signal attenuation. These results assume that the event propagates across the array as a plane wave. Practical departures from this idealized assumption may lead to results inconsistent with this type of analysis.

Table III-1 gives the great circle and on-line beam azimuths along with the peak amplitude attenuation measurements for each of the events. The numbers given are the ratios of off-line beam peak amplitude to on-line beam peak amplitude, expressed in dB. In all cases excepting KUR/219/13AL, the differences between the two beams exceeded two dB only where the signal-to-noise ratio was low. In other words, when the signal was large enough to be clearly measureable the difference between the two beams was two dB or less. In the case of the exception, KUR/219/13AL, the on-line beam shows a large pulse near the onset of the vertical component Rayleigh-wave. If the beam measurement is made on this pulse the on-line beam appears 4.3 dB larger than the off-line beam. It is possible, however, that this pulse is anomalous.

In some cases when the separation between great circle and on-line beam azimuths is large some crosstalk between the horizontal components is observed, i.e. the Love-wave appears on the radial component or vice versa. If the Love-wave and horizontal Rayleigh-wave have about the same amplitudes this does not appear noticeable in the amplitude measurements, but might be significant in the case of a large Love-wave.

There is little reason to believe that departure of the on-line beams from the great circle azimuth will consistently degrade the noise suppression of the beam. In light of the results above, it would appear that the practice of spacing on-line beams at 60° intervals results in adequate coverage with the subarray considered. This is particularly true of the vertical component where inter-mode crosstalk does not occur. A similar comparison with the full array will be made when appropriate data become available.

## E. Two-Component Rayleigh Wave Processing

Two-component Rayleigh wave processing consists of phase-shifting the in-line horizontal beam by $90^{o}$, applying a scale factor based on the ratio of vertical-to-horizontal RMS signal levels, and stacking the vertical and equalized horizontal beams. In this study 6 events and 19 noise samples (Table III-2) were processed over 4 bandwidths and two scale factors to determine the noise suppression and signal enhancement achieved by two-component processing. The bandwidths used were the following:

0.020 Hz to 0.060 Hz

0.020 Hz to 0.047 Hz

0.027 Hz to 0.060 Hz

0.027 Hz to 0.047 Hz

The two horizontal scale factors were 1.0 and 1.2.

The measure of the average increased noise suppression was obtained by comparing the integrated power spectra (at each bandwidth and scale factor) of the two-component processed noise with that of the beamsteered vertical component. The power values of these differences in dB are given in Table III-3.

In the case where the vertical and in-line horizontal beams had the same noise power density and were incoherent, noise rejection would be 1.3 dB ($\sqrt{N}$). On the average, two-component processing with a scale factor of 1.2 yields only slightly greater noise rejection than the 1.3 dB figure, while a scale factor of 1.0 gives from 0.7 to 1.0 dB greater rejection than the 1.3 dB figure. Perhaps even more significant is the average noise suppression obtained by two-component processing relative to the smaller of the vertical and in-line Rayleigh wave components (Table III-4). The average noise rejection using a scale factor of 1.0 is almost one dB greater than using a scale factor of 1.2, at

| Associated Event Name | No. of Sites | Date/ Hour of Event | Date/ Hour of Noise Sample | $M_s$ | $m_b$ |
|---|---|---|---|---|---|
| IRA/242/16* | 6 | 242/1600 | 242/1500 | 4.1 | 5.1 |
| CHI/220/11* | 5 | 220/1100 | 220/1000 | 4.0 | 4.7 |
| IRA/211/13 | 6 | 211/1300 | 211/1000 | — | — |
| CRS/287/06* | 7 | 287/0600 | 287/1300 | 4.6 | 6.7 |
| KYU/207/07* | 8 | 207/0700 | 207/0600 | 5.8 | 6.1 |
| GRC/184/00 | 6 | 184/0000 | 184/0300 | 3.9 | 5.1 |
| CHI/212/13* | 6 | 212/1300 | 212/1200 | 4.5 | 5.5 |
| KAM/242/00* | 7 | 242/0000 | 241/2300 | 4.8 | 5.2 |
| KAM/231/09 | 9 | 231/0900 | 234/1000 | 3.1 | 4.7 |
| KAM/285/22 | 7 | 225/2200 | 225/2100 | 3.3 | 4.6 |
| BUR/225/07 | 9 | 225/0700 | 225/0300 | 3.7 | 4.7 |
| KAM/242/03 | 6 | 242/0300 | 241/2200 | 3.6 | 4.8 |
| KAM/242/07 | 9 | 242/0700 | 242/0600 | 2.6 | 3.8 |
| CAU/243/04 | 7 | 243/0400 | 243/1200 | 3.0 | 4.0 |
| ALB/241/10 | 9 | 241/1000 | 241/0800 | 3.3 | 4.4 |
| SIN/240/05 | 6 | 240/0500 | 240/0000 | — | — |
| WKZ/357/07 | 7 | 357/0700 | 357/0600 | 4.3 | 6.1 |
| EKZ/351/07 | 6 | 351/0700 | 351/0600 | 3.3 | 5.3 |
| EKZ/147/07 | 3 | 147/0700 | 147/0300 | — | — |

* Events used in the signal enhancement study

TABLE III-2

19 EVENTS AND ASSOCIATED NOISE SAMPLES USED IN EVALUATION OF TWO-COMPONENT PROCESSING

| Associated Event Name | Improvement Of Two-Component Over Vertical Trace (dB) | | | | | | | |
|---|---|---|---|---|---|---|---|---|
| | 0.020 to 0.060 Hz Scale Factor | | 0.020 to 0.047 Hz Scale Factor | | 0.027 to 0.060 Hz Scale Factor | | 0.027 to 0.047 Hz Scale Factor | |
| | = 1.0 | = 1.2 | = 1.0 | = 1.2 | = 1.0 | = 1.2 | = 1.0 | = 1.2 |
| IRA/242/16 | 2.5 | 1.4 | 1.4 | 0.3 | 3.3 | 2.4 | 1.7 | 0.8 |
| CHI/220/11 | 2.8 | 2.1 | 2.0 | 1.1 | 3.6 | 2.9 | 2.7 | 1.9 |
| IRA/211/13 | 0.7 | -0.1 | 0.4 | -0.5 | 1.8 | 0.8 | 1.5 | 0.6 |
| KYU/207/07 | 3.3 | 2.6 | 3.8 | 3.0 | 2.9 | 2.2 | 3.5 | 2.9 |
| CRS/287/06 | 2.2 | 1.2 | 2.2 | 1.2 | 1.8 | 0.7 | 1.6 | 0.5 |
| GRC/184/00 | 1.4 | 0.0 | 0.8 | -0.6 | 1.5 | 0.4 | 0.6 | -0.5 |
| CHI/212/13 | 3.1 | 2.4 | 3.0 | 2.3 | 2.7 | 1.9 | 2.5 | 1.7 |
| KAM/242/00 | 1.9 | 0.9 | 1.6 | 0.6 | 2.5 | 1.7 | 2.2 | 1.4 |
| KAM/231/09 | 1.8 | 1.0 | 2.2 | 1.3 | 2.1 | 1.3 | 2.5 | 1.7 |
| KAM/225/22 | 5.3 | 4.5 | 5.6 | 5.0 | 4.3 | 3.4 | 4.7 | 4.1 |
| BUR/225/07 | 1.6 | 0.7 | 1.4 | 0.4 | 2.0 | 1.2 | 1.8 | 0.9 |
| KAM/242/03 | 2.9 | 2.1 | 3.9 | 3.2 | 2.2 | 1.4 | 3.1 | 2.4 |
| KAM/242/07 | 1.0 | -0.1 | 0.9 | 0.0 | 1.3 | 0.2 | 1.3 | 0.5 |
| CAU/243/04 | 1.9 | 1.0 | 1.6 | 0.7 | 2.1 | 1.4 | 1.5 | 0.7 |
| ALB/241/10 | 2.3 | 1.4 | 1.4 | 0.4 | 2.4 | 1.6 | 1.1 | 0.1 |
| SIN/240/05 | 1.5 | 0.6 | 1.2 | 0.0 | 1.9 | 1.1 | 1.2 | 0.1 |
| WKZ/357/07 | 1.4 | 0.6 | 1.2 | 0.4 | 1.3 | 0.4 | 1.1 | 0.2 |
| EKZ/351/07 | 2.6 | 1.8 | 2.5 | 1.6 | 3.3 | 2.3 | 3.9 | 2.9 |
| EKZ/147/04 | 3.1 | 2.2 | 2.8 | 1.7 | 2.5 | 1.5 | 1.6 | 0.5 |
| AVERAGE | 2.3 | 1.4 | 2.1 | 1.3 | 2.3 | 1.8 | 2.1 | 1.2 |

TABLE III-3

NOISE SUPPRESSION ACHIEVED BY TWO-COMPONENT PROCESSING

| Bandwidth (Hz) | Scale factor for the Horizontal Component | Average Noise Suppression (dB) | Difference In Achieved Noise Suppression (Scale factor = 1.2) - (Scale factor = 1.0) |
|---|---|---|---|
| 0.020-0.060 | 1.0 | 1.9 | -0.9 |
| 0.020-0.060 | 1.2 | 1.0 | |
| 0.020-0.047 | 1.0 | 1.6 | -0.8 |
| 0.020-0.047 | 1.2 | 0.8 | |
| 0.027-0.060 | 1.0 | 2.0 | -0.8 |
| 0.027-0.060 | 1.2 | 1.1 | |
| 0.027-0.047 | 1.0 | 1.6 | -0.9 |
| 0.027-0.047 | 1.2 | 0.7 | |

TABLE III-4

AVERAGE TWO-COMPONENT NOISE REJECTION IMPROVEMENT RELATIVE TO THE SMALLER OF VERTICAL AND HORIZONTAL COMPONENTS

all bandpasses. The scale factor of 1.0 achieves noise suppression of from 0.3 to 0.7 dB beyond the level expected for incoherent noise where the input noise level equals the lower of the vertical and in-line horizontal noise levels.

The signal gains (Table III-5) were obtained by taking the ratio of the maximum peak amplitude of the wideband processed two-component output and the amplitude of the wideband vertical Rayleigh wave at the same frequency. The signal-to-noise ratio improvement (Table III-5) was calculated as the difference in peak signal amplitude over RMS noise between the two-component processor output and the vertical Rayleigh wave. The two-component processor is slightly more effective when the bandpass is extended to 0.06 Hz on the high frequency end than when it is cut off at 0.047 Hz. This improved signal-to-noise ratio enhancement results from greater noise suppression at the higher frequencies as seen by the averages of Table III-3. In most cases the microseismic noise at ALPA propagates as surface waves coming from the South. Since the signals of Table III-5 tend to come from the North, the processor can reject the microseismic Rayleigh-wave noise by more than the 1.3 dB $\left(\sqrt{N}\right)$ figure. This capability is noted when the bandpass is extended to include the microseisms.

Scaling the horizontal trace by 1.0 yields slightly better results than the use of the 1.2 scalar. Apparently increasing the value to 1.2 increases the noise level more than the signal level in the processor output.

These results indicate that the 0.025 to 0.055 Hz bandpass previously selected for array processing and matched filtering is also suitable for two-component processing. The two-component processor achieves about two dB signal-to-noise ratio enhancement over the bandpassed vertical component beam.

| Event Name | Signal Gain | | Signal-to-noise Ratio Enhancement By Two-Component Processing (dB) | | | | | | | |
|---|---|---|---|---|---|---|---|---|---|---|
| | | | 0.020 to 0.060 Hz | | 0.020 to 0.047 Hz | | 0.027 to 0.060 Hz | | 0.027 to 0.047 Hz | |
| | Scale Factor | | Scale Factor | | Scale Factor | | Scale Factor | | Scale Factor | |
| | =1.0 | =1.2 | =1.0 | =1.2 | =1.0 | =1.2 | =1.0 | =1.2 | =1.0 | =1.2 |
| IRA/242/16 | 1.8 | 1.9 | 0.6 | 0.2 | -1.6 | -2.0 | 0.6 | 1.0 | -1.2 | -1.5 |
| CHI/220/11 | 2.2 | 2.3 | 3.5 | 1.7 | 2.0 | 0.7 | 3.8 | 2.1 | 2.9 | 2.2 |
| CRS/287/06 | 2.0 | 2.0 | 1.1 | 0.6 | 1.8 | 1.6 | 1.1 | 0.6 | 1.4 | 0.0 |
| KYU/207/07 | 2.0 | 1.8 | 2.2 | 1.8 | 3.1 | 3.0 | 2.0 | 1.3 | 2.7 | 2.7 |
| CHI/212/13 | 2.3 | 2.4 | 3.6 | 3.6 | 3.2 | 3.0 | 3.0 | 3.2 | 2.5 | 2.6 |
| KAM/242/00 | 2.2 | 2.1 | 1.9 | 1.6 | 0.6 | 0.2 | 2.5 | 2.6 | 1.3 | 0.1 |
| AVERAGE | | | 2.0 | 1.6 | 1.5 | 1.3 | 2.2 | 1.8 | 1.6 | 1.2 |

TABLE III-5

SIGNAL GAINS AND SIGNAL-TO-NOISE RATIO ENHANCEMENT FOR TWO-COMPONENT RAYLEIGH WAVE PROCESSING

## F. FUTURE PLANS

Routine processing of events with a two to three month lag between the time of occurence and the processing of the events. This lag ensures that PDE information is available prior to processing of the data. When the full array data become available the events will be processed with all available sites and with a seven site subarray. This will permit assessment of the relative capabilities of the two arrays. As events are processed, those suitable for use as master waveforms will be retained for this purpose.

Routine analysis of noise samples spaced at ten day intervals will continue. It is contemplated that this can be done most efficiently in batches covering two or three month intervals.

# IV. NORSAR LONG-PERIOD EVALUATION

## A. Introduction

The evaluation effort during the second quarter has been directed toward obtaining and processing the first large suite of events and noise samples. Fourteen events were edited and are now in analysis; event processing almost has been completed. Also, eleven noise samples, including two long-duration ( $>$3 hours) samples, have been obtained and processing is almost complete. A larger set of events would have been processed except that an unusually large amount of time was spent finding and editing suitable data. The NORSAR array was just becoming operational during this period.

Results of the evaluation to date are presented in the following sections. Section B reviews data quality; section C discusses signal analysis; section D discusses the ambient noise field; section E discusses some initial results from the array processing task; section F presents the first results of chirp filtering the array output beams. No information on NORSAR long-period detection capability or discrimination capability is yet available; preliminary data on these topics will be obtained in the near future.

## B. General Data Quality

The small amount of data processed during this quarter reflects the difficulty encountered in obtaining good data. This difficulty is primarily the result of non-continuity in time of the data (mostly caused by transmission problems) and incomplete event information.

Events edited during this quarter were obtained from the interval day 168 to day 216 (17 June to 4 August, 1971). Since available "PDE" bulletins only covered the first part of this period the SAAC bulletins were the primary source of event information. The total number of events from the Eurasian landmass (including Russia but excluding East and West Europe) given by the SAAC bulletin was 123.

Since this was preliminary analysis, we chose only those events which were either visible on the raw data or which were from areas of interest and listed by PDE. Of these 123 events only nine contained both visible surface waves and reasonably continuous time data. Actually, twelve events were processed since three others from areas of interest were listed by PDE . A breakdown of the reasons these 114 events were initially rejected is as follows:

- data was not available for 43 events (NDPC data was not present on the SAAC library tapes for the period from day 174 to day 183)
- 28 events had large time gaps in the data which precluded analysis
- 4 events were definitely interfered with by other events (interfering events listed by SAAC)
- 14 events appeared to be interfered with by other events
- 5 events had uncorrectable amplitude spikes occuring in the surface wavetrain
- 13 events were not visible (three were subsequently confirmed by PDE and were then used)
- 5 events were mislocated by SAAC
- 1 event was too deep to be of interest
- 1 event occurred when the data on all sites and components was identical

Almost all of the data not rejected due to time gaps contained some of these gaps. When the gaps were not excessive or if they were not present in the surface wave trains, the data were processed with allowances made for the missing time.

Contrary to our original suspicions, data dropout now appears to be mostly random and unrelated to any seismic wave arrivals at NORSAR. Information on the dropout rate is now available but has not yet been tabulated. The ten day loss of data apparently was due to an undetected transmission failure. It is believed that operational procedures at SAAC have been revised to prevent a recurrence of this type of data loss. Another source of data loss is use of the TAL for vocal communication with NDPC (data cannot be transmitted when the modem is in voice mode). The amount of data lost from this cause has not been investigated; however, communication to NDPC via the computer console typewriter should be used whenever possible to prevent interruption of the data.

C. Signal Analysis

During this quarter, four additional events with large S/N ratio were edited for signal analysis. The six events presently being analyzed are listed in Table IV-1.

This analysis consists of determining signal characteristics that will affect array processing. The questions to be answered are:

- Are the signals similar at each site?
- Do events arrive along the great circle route and at the expected times?
- What is the spectral content of the signals and the variation by region?
- What is the signal duration?
- Are there multipathed arrivals and what are the secondary arrival directions?

Signal similarities have been measured for all six events. Table IV-2 presents the average similarity (correlation coefficient) between the reference

TABLE IV-1

LIST OF EVENTS FOR SIGNAL ANALYSIS

| Date | Time (GMT) | Latitude | Longitude | $m_b$ | Area | Name |
|---|---|---|---|---|---|---|
| May 6 | 04.24.33.9 | 39.0N | 29.7E | 4.6 | Turkey | TUR/126/04NL |
| May 23 | 01.02.54 | 37.6N | 30.1E | 4.4 | Turkey | TUR/143/01NL |
| June 10 | 09.31.54.5 | 39.1N | 29.6E | 4.9 | Turkey | TUR/161/09NL |
| July 9 | 16.44.15.8 | 43.5N | 147.7E | 4.9 | Kuriles | KUR/190/06NL |
| July 27 | 12.48.24 | 39.0N | 78.0E | 5.3 | Sinkiang | CHI/208/13NL* |
| August 1 | 02.06.06.6 | 50.4N | 156.8E | 5.6 | Kuriles | KUR/213/02NL |

* Event not yet verified by PDE information

TABLE IV-2

SIGNAL SIMILARITY

| Event | S vertical | S radial | LQ transverse | LR vertical | LR radial |
|---|---|---|---|---|---|
| TUR/161/09NL | 0.840 | 0.906 | 0.916 | 0.893 | 0.836 |
| TUR/143/01NL | 0.921 | 0.900 | 0.867 | 0.863 | 0.810 |
| TUR/126/04NL | 0.969 | 0.923 | 0.950 | 0.885 | 0.836 |
| KUR/190/16NL | ——— | ——— | 0.813 | 0.815 | 0.792 |
| KUR/213/02NL | 0.917 | 0.930 | 0.890 | 0.884 | 0.869 |
| CHI/208/13NL | ——— | ——— | 0.907 | 0.929 | 0.898 |

site and the other sites for the vertical and radial S, transverse Love and vertical and radial Rayleigh modes. As can be seen, the coefficients are above 0.80 indicating good similarity across the array.

Power spectra were also generated for each event, and Figures IV-1, IV-2 and IV-3 show spectra from three different areas. The locations of the three Turkish events are very close. TUR/126/04NL and TUR/161/09NL are within 0.1 degrees of each other and their spectra are nearly identical. The spectra for TUR/143/01NL (Figure IV-1) which is approximately 3.5 degrees from the other two, is essentially the same as the others although the width of the -6 dB band (6 dB down from the peak power) for the vertical component is narrower (0.025 Hz - 0.06 Hz for TUR/143/01NL versus 0.025 Hz - 0.070 Hz for TUR/126/04NL).

The Kurile events are separated by fourteen degrees however, they both peak at 0.040 Hz on the verticals and the widths of the -6 dB band for the verticals are the same (0.025 Hz to 0.060 Hz).

The Chinese event CHI/208/13NL has more high frequency energy than the other events (width of the -6 dB band is 0.040 Hz to 0.070 Hz) and the vertical peak is 0.055 Hz.

In order to determine the optimum passband for more routine processing, the bandwidth behavior of many events from different regions must be observed. If significant signal energy is present at higher frequencies for events from some regions, passbands tailored for each region may be necessary.

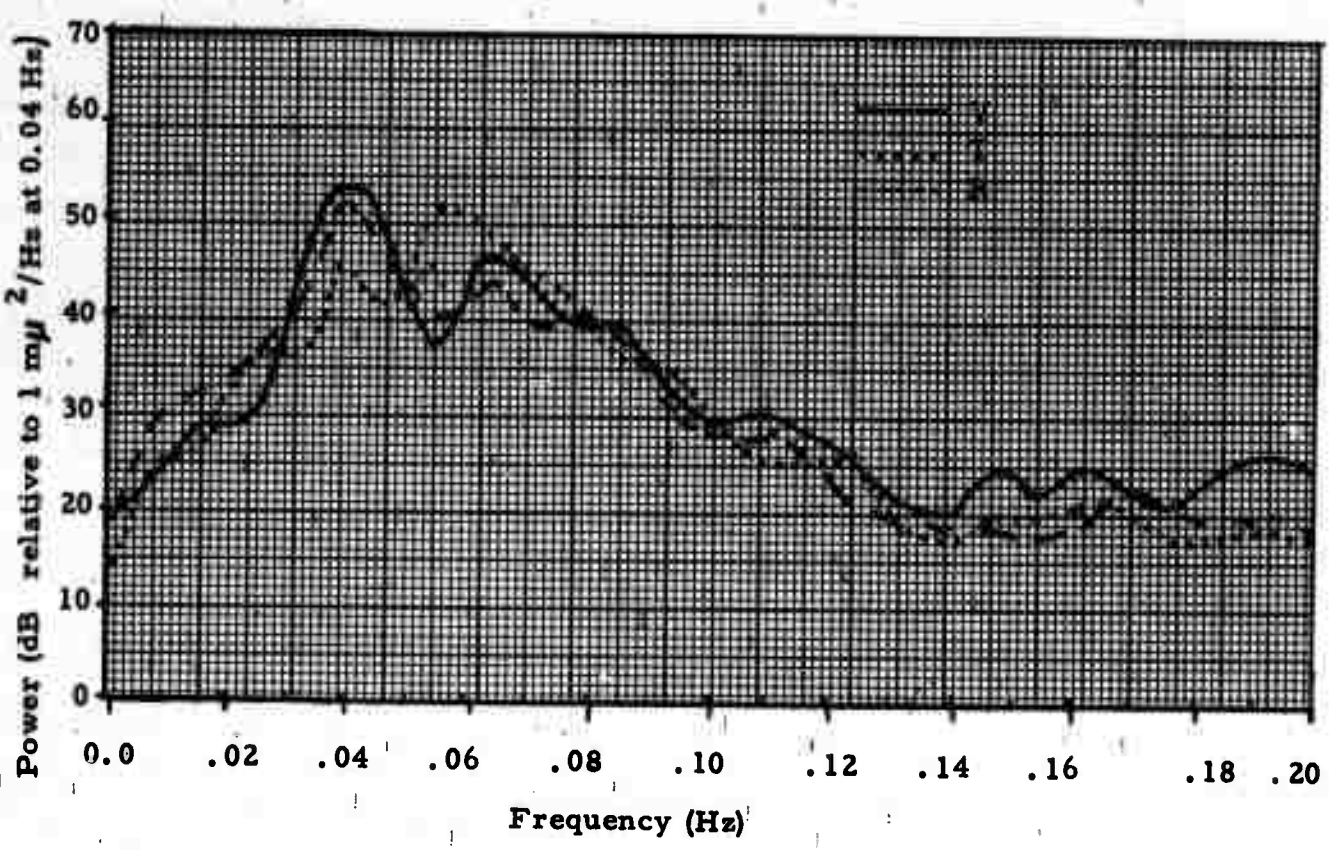


FIGURE IV-1

3 COMPONENT POWER SPECTRA FOR EVENT TUR/143/01NL
SITE 3

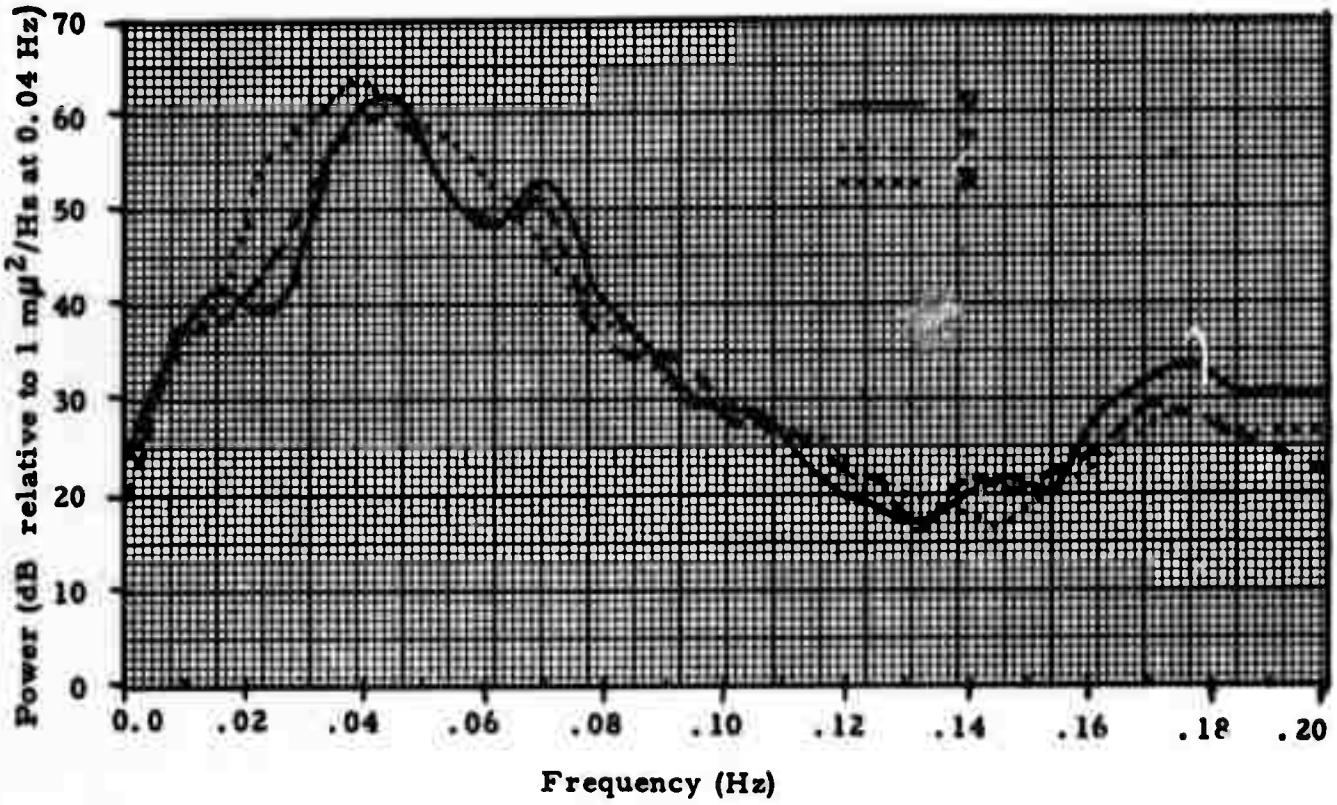


FIGURE IV-2

3 COMPONENT POWER SPECTRA FOR EVENT KUR/190/16NL
SITE 3

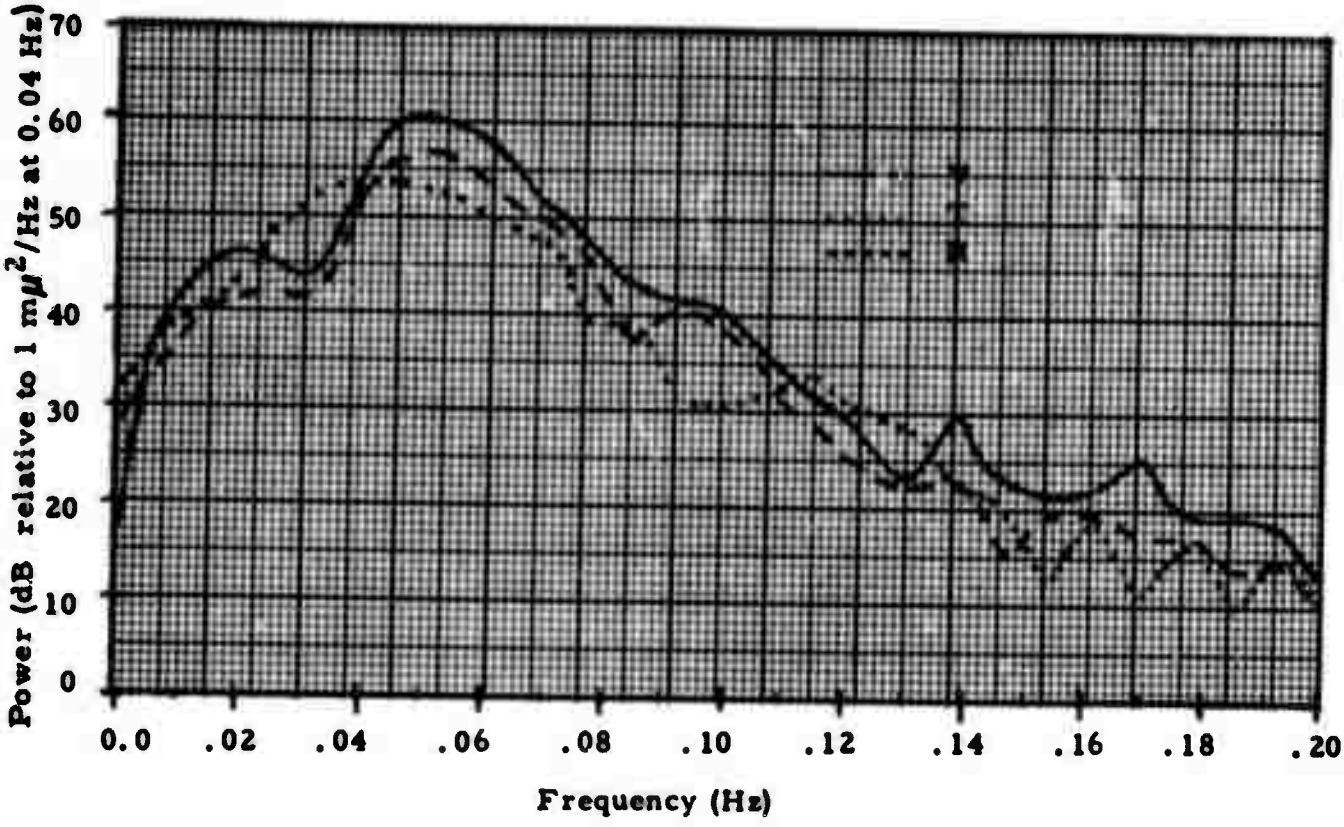


FIGURE IV-3

3 COMPONENT POWER SPECTRA FOR EVENT CHI/208/13NL
SITE 3

D. Noise Analysis

A preliminary analysis of the NORSAR long-period noise was conducted using ten noise samples taken at approximate ten day intervals during the period from day 121 to day 220 (May 1, 1971 to August 8, 1971) Table IV-3 is a list of the noise samples and their lengths.

A typical 3-component noise power density spectrum is shown in Figure IV-4. The system response is not removed, but the spectrum is normalized to 1 $m\mu^2$/Hz at 0.04 Hz. The 16-18 second microseismic peak dominates the spectrum with levels at 30 to 40 dB. There is generally a small notch between .090 and 0.10 Hz (10-11 seconds). The three components are generally within 3 dB from 0.047 to higher frequeicies.

Below the microseismic peak long-period noise often appears on the horizontals (Figure IV-5). The long-period horizontal noise is highly variable from site to site and is observed in the signal processing band (20-40 second periods). Figure IV-6 shows the variations of the RMS ground motion in the 20-40 second period band as a function of site. As can be seen, the horizontal RMS values fluctuate considerably more than the vertical values (9 dB vs 3 dB). At the microsesimic peak noise levels are reasonably similar across the array and among components (Figure IV-7). To date no frequency response calibrations have been available, however, the small variation in microseismic peak noise level indicates reasonably good equalization between sites.

The 20-40 second array average RMS noise levels were plotted versus time to investigate time variability of the NORSAR long-period noise field, (Figure IV-8). The fluctuations in the horizontal noise level is seen to be much larger than the vertical noise (12 dB maximum), but no long term trend is indicated. RMS levels in this band ranged from 5 to 12 $m\mu$ for the vertical, 6 to 20 $m\mu$ for the North-South, and 5 to 15 $m\mu$ for the East-West. These values are similar to those observed at ALPA.

TABLE IV-3
NORSAR NOISE SAMPLES

| DAY | LENGTH |
|---|---|
| 121 | 39m-24 sec |
| 135 | 1hr-33m-52sec |
| 141 | 1hr-16m-48sec |
| 150 | 57m-28sec |
| 164 | 4hr-37m-20sec |
| 171 | 1hr-16m-48sec |
| 191 | 51m-12sec |
| 201 | 59m-44sec |
| 211 | 1hr-12m-32sec |
| 220 | 4hr-24m-32sec |

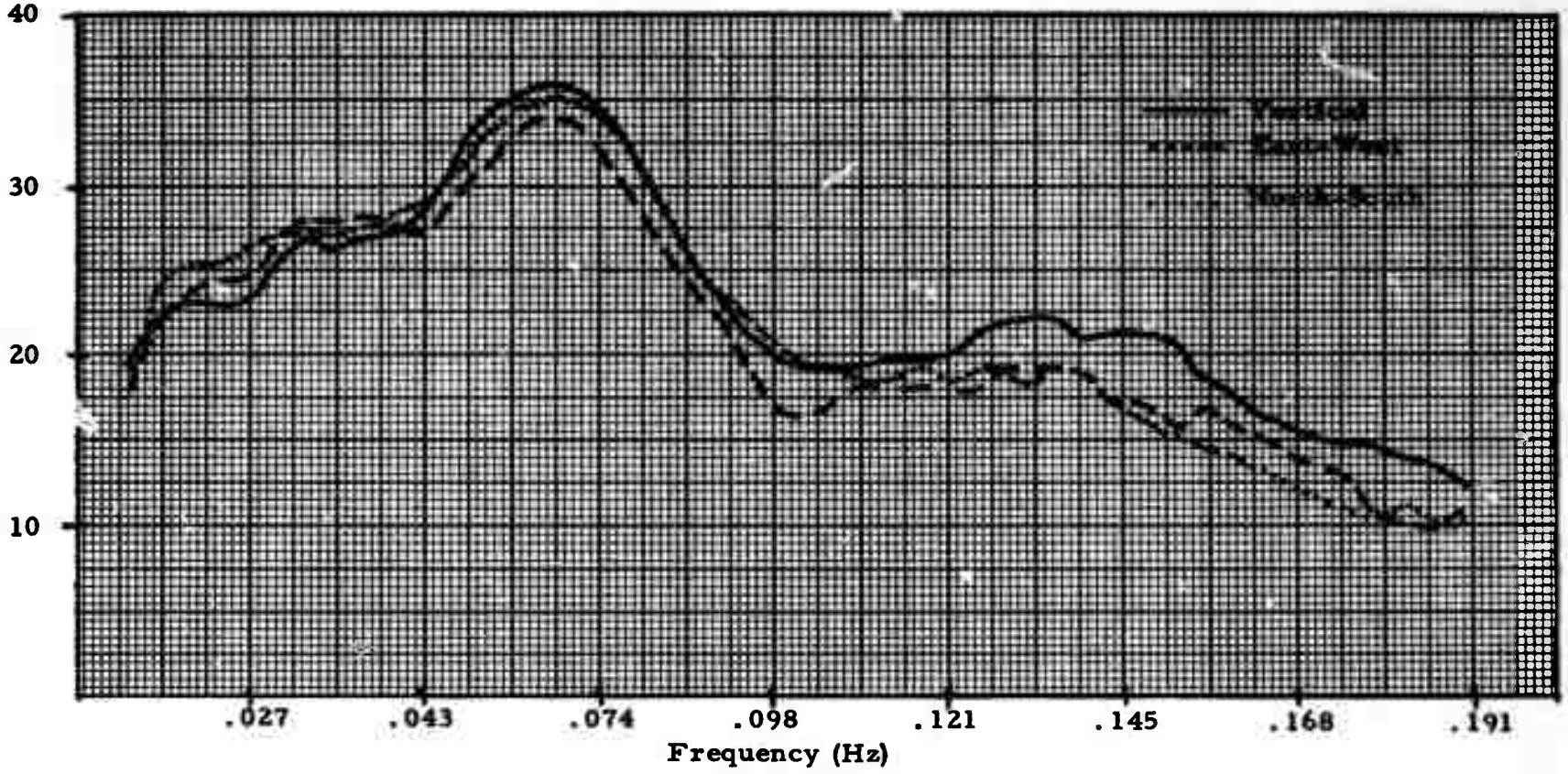


FIGURE IV-4

TYPICAL NOISE POWER SPECTRA DAY 220 SITE 4

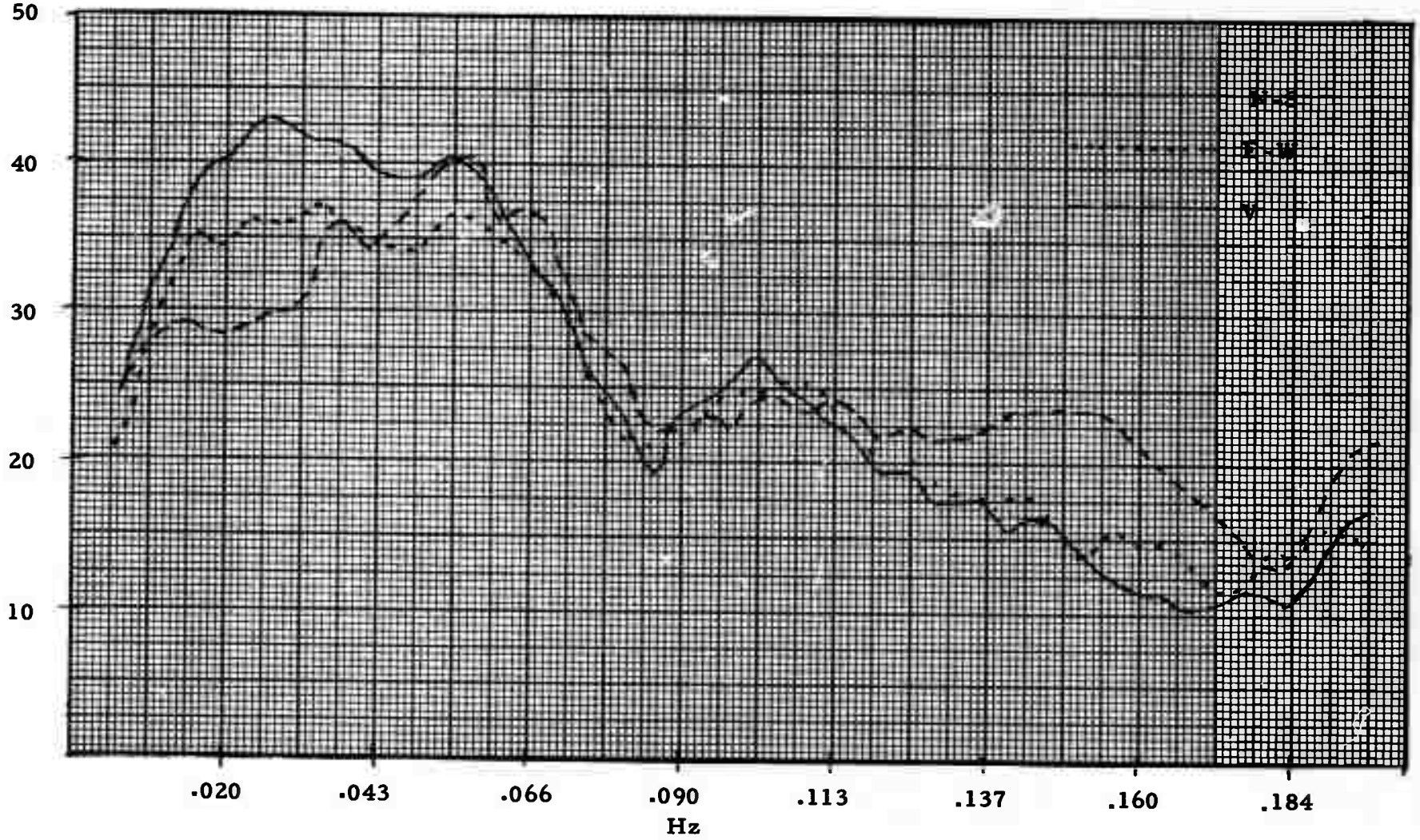


FIGURE IV-5

EXAMPLE OF STRONG LONG PERIOD ENERGY ON HORIZONTALS

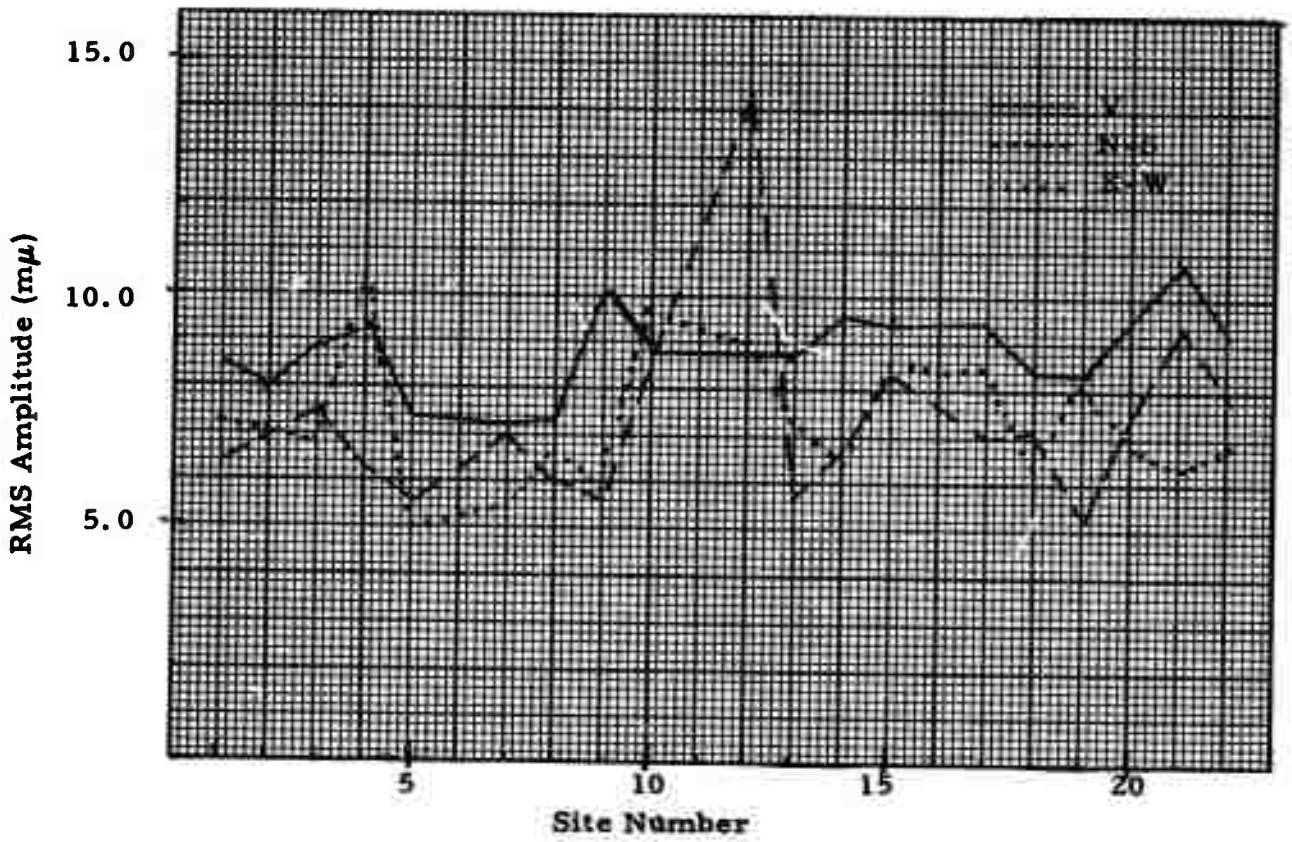


FIGURE IV-6

VARIATION OF RMS GROUND MOTION (20-40sec) vs. SITE ON DAY 201

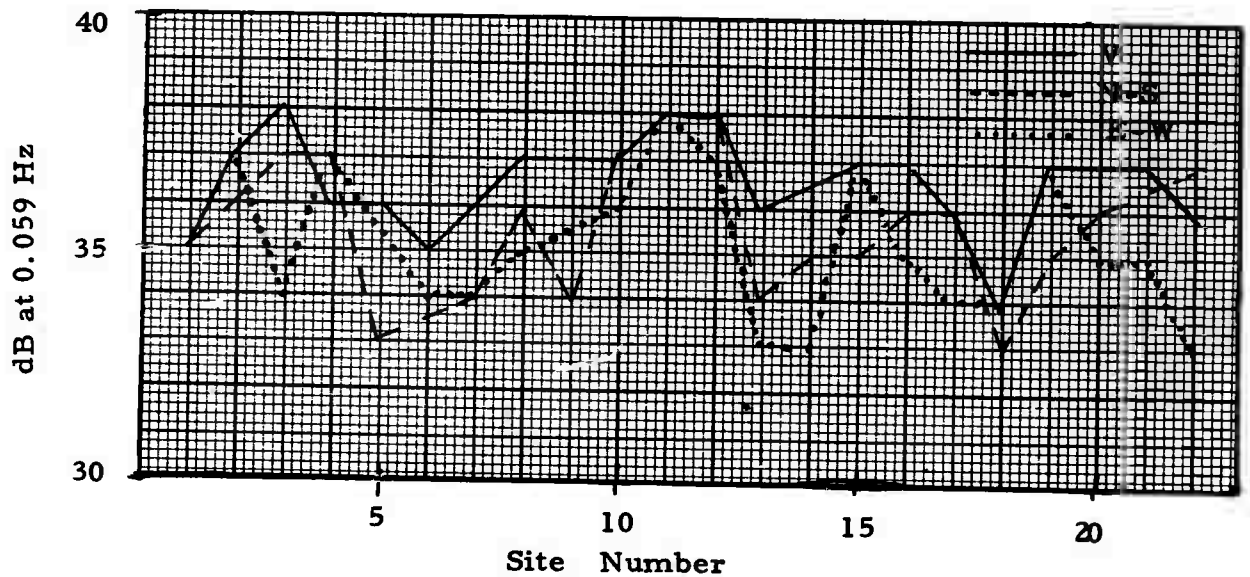


FIGURE IV-7

POWER DENSITY SPECTRA AT 0.059 Hz BY SITE DAY 211

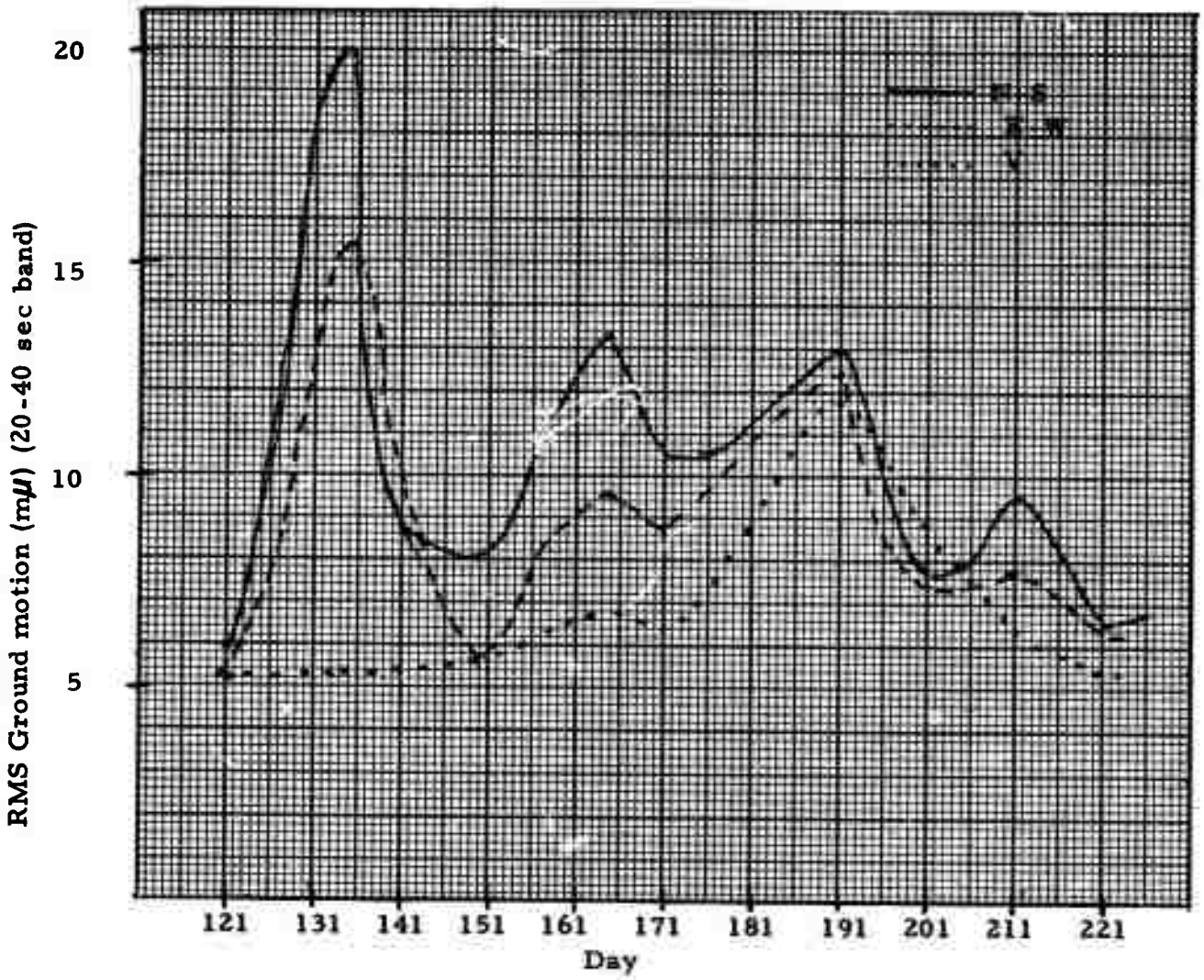


FIGURE IV-8

VARIATION OF AVERAGE 20-40 sec. RMS GROUND MOTION FROM DAY 121 TO DAY 221 FOR THREE COMPONENTS

Figures IV-9 and IV-10 show the multiple coherence of the two four hour samples at day 164 and day 220 for all three components. The dots above the curves indicate the peaks in the power density spectrum at these days. Figure IV-9, for day 164, shows the two noise power density spectrum peaks (at 16-18 seconds and 8.5 seconds) to be fairly coherent on the vertical (0.9 and 0.8 respectively) but only moderately coherent on the horizontals ( in fact the East-West component does not have an 8 second period peak). The noise sample shows low coherence at periods below the microseismic peak between .07 to 0.10 Hz.

Figure IV-10, for day 220, shows a generally broader coherent peak of about 0.9 on all three components between 0.05 and 0.08 Hz. The null at 0.07 to 0.10 Hz seen on day 164 is not present here (there was no null in the power density spectra for this day). The coherence above 0.08 Hz generally drops with increasing frequency, although there is a "plateau" in the vertical coherence between 0.08 and 0.15 Hz.

These coherence results are not encouraging with regard to multi-channel filtering; based on this very preliminary analysis it does not appear that multichannel filtering will significantly outperform beamsteering in noise rejection.

High resolution frequency-wavenumber spectra were calculated for all noise samples to determine direction and velocity of the coherent noise power spectra peaks. Table IV-4 shows the results of the vertical component for each noise sample. The most common propagation direction was $90^{\circ}$ to $100^{\circ}$, although noise appeared from every quadrant. Since the signals of interest will have azimuths from $0^{\circ}$ to $120^{\circ}$, the noise and signal will have similar azimuths in many cases and less than $\sqrt{N}$ array processing noise rejection might be expected for these cases.

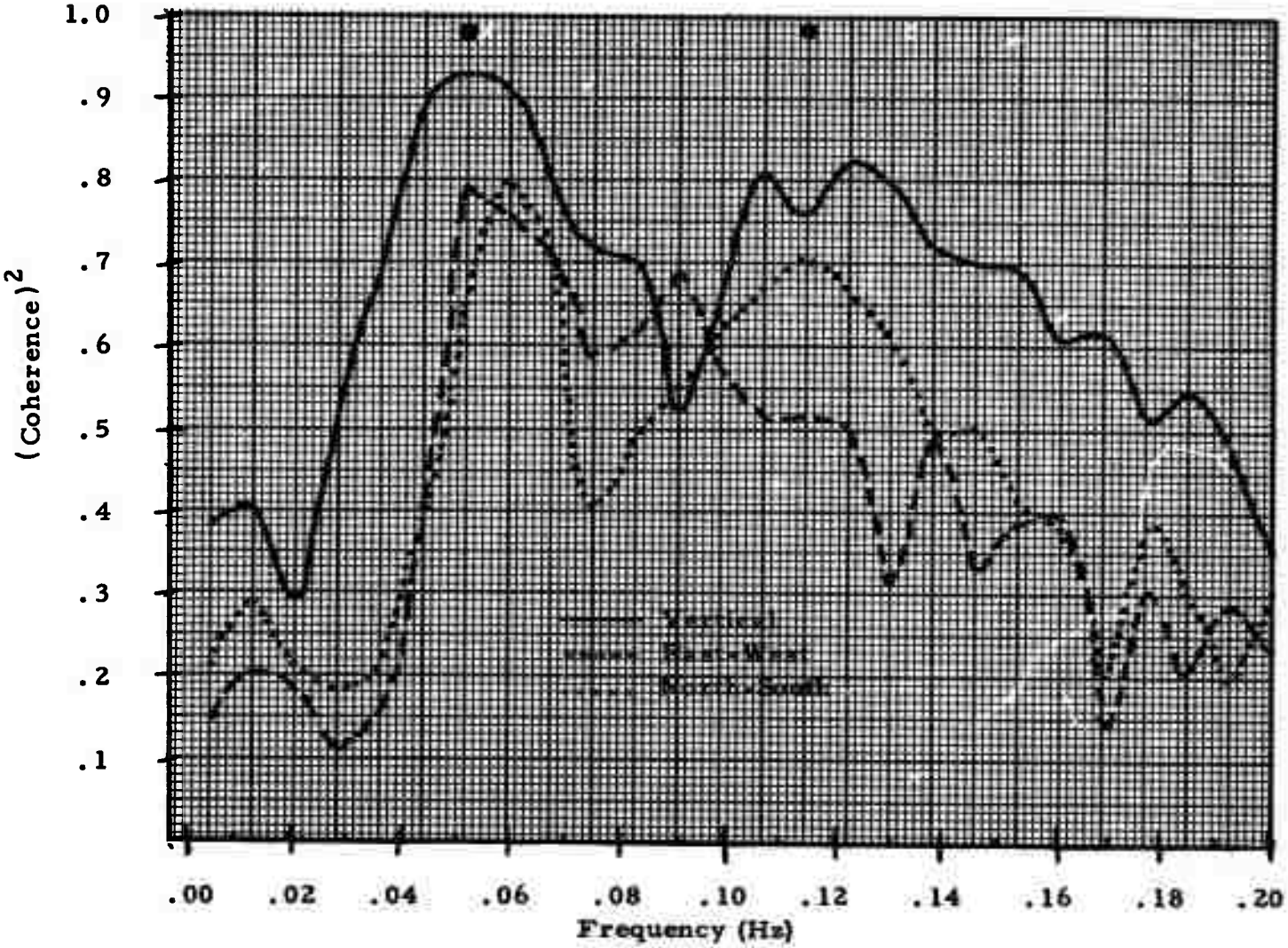


FIGURE IV-9

MULTIPLE COHERENCE DAY 164 SITE 1 PREDICTED FROM SITES 2, 3, 4, 7, 8, 9, 11, 13, 14, 15, 16, 17, 18, 19, 22

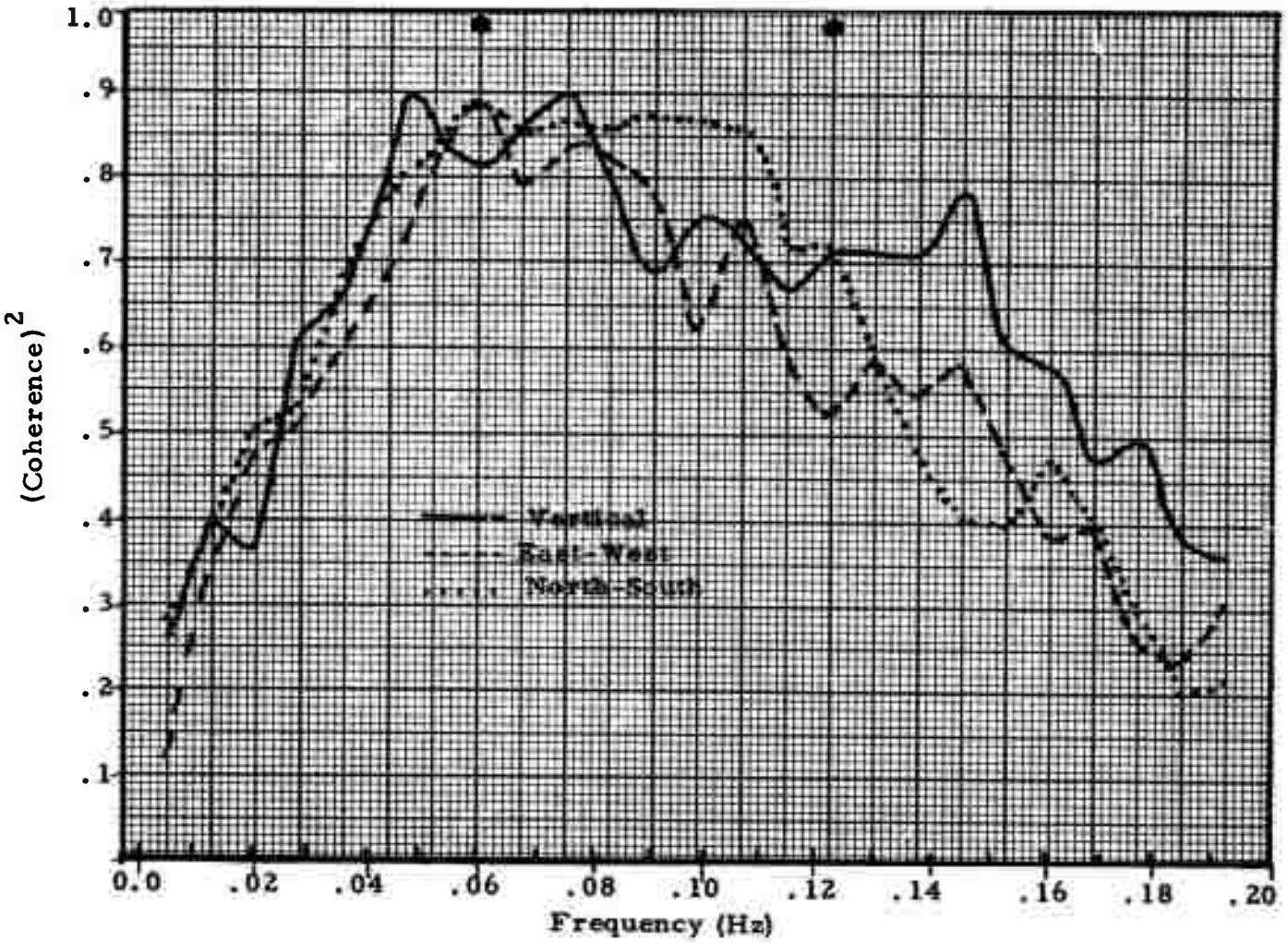


FIGURE IV-10

MULTIPLE COHERENCE DAY 220 SITE 1 PREDICTED FROM SITES
3, 4, 5, 6, 7, 8, 9, 10, 13, 14, 15,
16, 17, 18, 20, 22

TABLE IV-4

FREQUENCY, VELOCITY AND AZIMUTH OF NOISE SAMPLES

| Day | Frequency | Velocity | Azimuth |
|---|---|---|---|
| 121 | .059 | 3.6 | 197° |
| 135 | .059 | 3.8 | 92° |
| 141 | .055 | 3.8 | 108° |
| 150 | .066 | 3.6 | 5° |
| 164 | .059 | 3.8 | 240° |
| 171 | .051 | 3.7 | 195° |
| 191 | .051 | 3.7 | 90° |
| 201 | .059 | 3.7 | 60° |
| 211 | .059 | 3.8 | 100° |
| 220 | .059 | 3.7 | 303° |

## E. Array Processing Performance

This analysis is directed toward comparing the performance of conventional beamsteering and multichannel filtering (MCF) at NORSAR. The response of both processors to signals can be made to be essentially identical and so their performance can be compared in terms of their ability to suppress noise in the output beam.

Two long duration and one medium duration noise samples have been used for MCF design and testing. First, a portion of each sample was used to estimate a set of crosspower matrices, then a vertical component MCF was designed using a signal-to-noise ratio of 4.0 and a dispersive signal model steered to an azimuth of 76°. The beamsteer filter and the MCF were applied to two sections of the data. The first section, within the MCF design gate, produced the "on-design" output, and the second section, not used in the design gate, produced the "off-design" output. The amount of data for each sample used for this analysis are given in Table IV-5.

Input power was computed by averaging the vertical component power from each site used in the MCF design. The MCF and beamsteer filters utilized the same sites. The ratios of the average input power to the output power expressed in dB, for the MCF and beamsteer filter, in the frequency band of 0.023 to 0.051 Hz, are given in Table IV-6. These results are similar to those obtained from ALPA. Operating in the design gate, the MCF achieves 5.7, 2.7, and 0.8 dB of additional noise suppression over the beamsteer. Outside of the design gate, the relative performance drops 2.3, 0.5, and -1.3 dB. Note that in only one case (the MCF processor for day 164) was the $\sqrt{N}$ in noise rejection exceeded for off-design noise.

The degradation of MCF performance for off-design noise can be due to either insufficient statistics or non-stationarity of the noise. In two of the

TABLE IV-5

MCF AND BS FILTER DESIGN PARAMETERS

| Sample | Number Of Sites | Design Gate Duration (sec) | On-Design Duration (sec) | Off-Design Duration (sec) |
|---|---|---|---|---|
| NOIS/164 | 13 | 12800 | 5120 | 5120 |
| EKZ/145 | 16 | 5632 | 3072 | 3072 |
| NOIS/220 | 15 | 11520 | 5888 | 2816 |

TABLE IV-6

ARRAY PROCESSOR NOISE SUPPRESSION

| Noise In / Noise Out (dB) vertical component | | | | | |
|---|---|---|---|---|---|
| Sample | $\sqrt{N}$ Gain | On-Design | | Off-Design | |
| | | BS | MCF | BS | MCF |
| NOIS/164 | 11.1 | 7.2 | 12.9 | 9.3 | 11.6 |
| EKZ/145 | 12.0 | 7.6 | 10.3 | 5.8 | 6.3 |
| NOIS/220 | 11.8 | 10.0 | 10.8 | 9.2 | 7.9 |

three samples over three hours of noise were used to estimate the spectral matrices for considerably fewer than the full 22 sites potentially available and so the degradation in off-line performance is most likely due to the non-stationarity of the noise field. Based on these preliminary results, it does not seem likely that MCF processing will offer significant improvement relative to beamsteering at NORSAR. This task will be continued, however, with several more long noise samples so that a more definitive answer as to MCF effectiveness can be obtained.

### F. Matched Filter Performance

Chirp filter performance at NORSAR has been measured for nine Eurasian events listed in Table IV-7. The performance was measured by taking the ratio of the maximum amplitude of the chirp filter to the maximum amplitude of the array beam, after application of a bandpass filter with the same passband as the chirp. This measurement is valid because both the chirp and bandpass filter will have the same RMS noise output level. At the present time, the best passband for NORSAR has not been determined. It is likely that the band will be close to that for the ALPA; thus a .025 to .055 Hz band was selected for these events. The chirp filter length was chosen for each event after rough measurements of duration and dispersion were made on the waveforms. No master waveform filtering has been done yet; however, two events which have been chosen as masters have been matched against themselves.

The chirp filtering results to date are shown in Table IV-7 and the master events matched (and bandpassed) to themselves are shown in Table IV-8. The following observations may be made for this small ensemble:

- The Love wave gains are generally smaller than Rayleigh wave gains except for two Kurile events. These two appear to have the same source mechanism since their waveforms are almost identical point for point.

TABLE IV-7

CHIRP FILTER IMPROVEMENTS

| | | | Improvement Chirp/BP (dB) 0.025 - 0.055 Hz | | | |
|---|---|---|---|---|---|---|
| Event | $m_b$ | Δ | LQT | LRV | LRR | $M_s$ |
| KUR/190/16 | 4.9 | 69.9 | 6.4 | 3.9 | 5.3 | 4.8 |
| KUR/191/03 | 4.8 | 69.8 | 6.1 | 4.0 | 3.9 | 4.4 |
| KUR/191/09 | 4.6 | 69.2 | ND* | ND | ND | — |
| KUR/213/02 | 5.7 | 65.1 | 3.6 | 6.3 | 5.6 | 4.9 |
| SIB/212/01 | 3.5 | 55.3 | — | 2.5 | 0.7 | 3.4 |
| CHI/208/13 | 5.3 | 45.8 | 0.4 | 1.3 | 1.2 | 4.6 |
| BSA/210/19 | 4.5 | 22.2 | — | 0.3 | — | 2.8 |
| SRS/200/20 | 3.8 | 19.8 | -1.6 | 2.1 | 3.3 | 3.1 |
| WRS/191/17 | 5.3 | 20.3 | ND | ND | ND | — |

* Not Detected

TABLE IV-8

MASTER APPLIED TO MASTER IMPROVEMENTS

| Improvment (dB) 0.025 - 0.055 Hz | | | |
|---|---|---|---|
| Event | LQT | LRV | LRR |
| KUR/190/16 | 11.5 | 6.6 | 9.7 |
| CHI/208/13 | 4.7 | 3.5 | 4.5 |

- The waveform of the China event was not well dispersed and was of unusually short duration. Chirping would not be expected to be effective for that event.
- The radial and vertical component Rayleigh chirp improvements are close, as would be expected.
- The chirp filter lengths chosen may not be optimum in a few cases and some additional improvement may be available.
- The two events matched against themselves gave about 4 dB more improvement than that obtained by chirp filtering.

As the signal and noise structure become better defined it is expected that additional chirp improvement will be achieved. Some of the above events will be reprocessed to obtain any additional gain available.

G. Future Plans

During the third quarter, evaluation will be directed at further definition of array behavior with events of moderate magnitude. Definition of passband limits for event processing will have high priority. Reducing the number of trial bandpass filters used reduces proportionally the amount of processing time needed.

Noise analysis will continue with routine noise sample edits taken at approximately ten day intervals as well as edits of at least one long duration sample each month if data are available.

Chirp filtering will continue and matched filtering will be begun. A certain amount of reworking of the present suite of events is planned through further optimizing of the chirp results. Matched filtering with master waveforms will begin and standard discriminants will be computed.

The present goal for the number of new events to be editted and processed for the third quarter is at least 45. Whenever possible, the PDE bulletin will be used for event information, however the SAAC bulletin will be used for the lower magnitude events. Events with magnitudes between 4.0 and 5.5 will be of primary interest.

# V. NORSAR SHORT-PERIOD EVALUATION

The NORSAR short-period array is a 100-kilometer-diameter array with 22 subarrays each with 6 sensors. Every site is located within a different subarray of the short-period array. Each short-period subarray contains a central sensor surrounded by a 5-sensor ring appriximately 7 kilometers in diameter. In this section subarray 1 refers to subarray 1A, subarrays 2 through 8 to subarrays 1B through 7B, and subarrays 9 through 22 to subarrays 1C through 14C. Within a subarray, sensors 0 through 4 refer to sensors in the surrounding ring, starting at approximately $0^{o}$ relative to the central sensor of the subarray. Sensor 5 refers to the central sensor of the subarray. Thus sensor 0 of subarray 1 is sensor 01A01 in the official nomenclautre, and sensor 5 of subarray 22 is sensor 14C00.

NORSAR short-period array analysis effort to date has been concentrated in four areas:

- General quality of the 132 channel data
- Noise analysis
- Study of signal characteristics
- Determination of array beamforming techniques

Subsection A briefly covers the quality of data transcription for the NORWAY NDPC tapes. Subsection B describes highlights of noise analysis conducted on the 14 noise samples processed. Subsection C presents the results of signal analysis performed on selected events. Subsection D discusses attempts to improve beamforming performance through the determination of a set of adjusted propagation delays for different event epicenters and through the selective weighting of subarrays during array summation (using a diversity-stack technique).

A. Data Transcription Quality

Thus far, the NORSAR short-period edit program has attempted to transcribe 22 signals and a 5-minute noise sample preceding each signal from the NORWAY NDPC tapes. Fifteen signals and 14 noise samples were successfully edited. Table V-1 shows epicenter data for the 15 signals. No noise sample was obtained for Event 3. About one minute after the signal arrival for Event 3, 4 1/2 seconds of data were flagged as invalid and contained no valid seismic information. A tape dump of one of the 7 signal samples not successfully edited also showed that the data were flagged as invalid and contained no valid seismic information.

The 15 signals and 14 noise samples successfully edited appeared to have no recording problems with the exception that, in the case of 6 events, one subarray was down during both the signal and noise samples.

B. Noise Analysis

The noise analysis is based on 14 five-minute noise samples associated with the events of Table V-1 and covering the period 9 March 1971 to 3 May 1971. Because of the similarity of these samples, data from the sample associated with the Greece event has been used for display purposes.

The preliminary noise analysis has two basic objectives: the first is to examine the general data quality, the second is to examine noise characteristics as they affect array processing.

The following measurements were made to meet these objectives:

- Visual review of the data
- Single - sensor RMS levels
- Single - sensor spectra and spectral ratios
- Subarray beam spectra and spectral ratios
- Array beam spectra

TABLE V-1

EPICENTRAL DATA FOR NORSAR SIGNAL SAMPLES

| Event | Date | Origin Time | Latitude | Longitude | Depth | $m_b$ | Region |
|---|---|---|---|---|---|---|---|
| 1 | 3/9/71 | 04 58 38.9 | 38.7N | 20.3E | 16 | 4.8 | Greece |
| 2 | 3/13/71 | 23 51 35.5 | 50.6N | 129.9W | Normal | 5.7 | Vancouver Island |
| 3 | 3/23/71 | 06 59 56.0 | 61.3N | 56.5E | 0 | 5.6 | Ural Mountains |
| 4 | 3/23/71 | 09 52 12.3 | 41.5N | 79.3E | Normal | 5.7 | Kirgiz-Sinkiang Border |
| 5 | 3/23/71 | 20 47 17.4 | 41.5N | 79.3E | Normal | 6.0 | Kirgiz-Sinkiang Border |
| 6 | 3/24/71 | 20 54 28.6 | 41.5N | 79.5E | 18 | 5.3 | Kirgiz-Sinkiang Border |
| 7 | 4/3/71 | 07 34 50.2 | 32.2N | 95.1E | Normal | 5.1 | Tibet |
| 8 | 4/9/71 | 15 08 09.7 | 44.3N | 147.0E | 126 | 5.1 | Kurile Islands |
| 9 | 4/10/71 | 02 58 05.9 | 42.5N | 20.1E | 21 | 4.6 | Yugoslavia |
| 10 | 4/11/71 | 08 42 05.7 | 46.2N | 153.0E | Normal | 4.5 | Kurile Islands |
| 11 | 4/12/71 | 19 03 25.9 | 28.3N | 55.6E | 44 | 6.0 | Southern Iran |
| 12 | 4/18/71 | 23 14 19.0 | 45.8N | 76.1E | Normal | 4.5 | Eastern Kazakh SSR |
| 13 | 4/19/71 | 02 43 52.2 | 39.0N | 20.5E | 16 | 5.1 | Greece - Albania Border |
| 14 | 4/20/71 | 03 48 27.0 | 38.3N | 73.5E | 130 | 4.9 | Tadzkik-Sinkiang Border |
| 15 | 5/3/71 | 00 33 22.5 | 30.8N | 84.5E | 16 | 5.4 | Tibet |

- Multiple coherence within subarrays
- Multiple coherence between subarrays

A visual review of the noise data showed that there were no spikes, glitches, or other anomalies in the samples and that all traces appear to be "normal".

The single sensor RMS noise levels for each of the 132 sensors were calculated to determine the distribution of wide-band single sensor power. Figure V-1 is a histogram for the RMS power for the 132 data channels for the Greece noise sample and shows that the spread of RMS noise values is small, suggesting that the sensors are well equalized and the absolute noise level is rather constant over the array. Figure V-2 is the corresponding histogram for a noise sample taken before event 11 from Southern Iran. The spread of RMS values is similar to that shown in Figure V-1. RMS values before event 8 from the Kurile Islands showed an even smaller spread.

The single sensor power spectra and variations in these spectra were examined next. The characteristics of the single sensor and array noise field are summarized in Figure V-3, which shows the average single sensor spectrum, array beam spectrum, and the spectral ratio of the array beam to the average single sensor spectrum for the Greece sample. No instrument response corrections have been made to these data. Also, the spectra are not absolute. The noise spectra are very simple, with a peak at .16 to .33 Hz (6 to 3 second period) and a very rapid decrease in spectral density with increasing frequency. Note that the array beam achieves $\sqrt{N}$ noise rejection over the entire 0 to 5 Hz band.

The single sensor power spectra variations are summarized in Figure V-4, which shows a typical sensor to average single sensor spectral ratio, the maximum positive ratio (sensor 3 of subarray 10) and the maximum negative ratio (sensor 2 of subarray 11). Figure V-4 shows that the 132

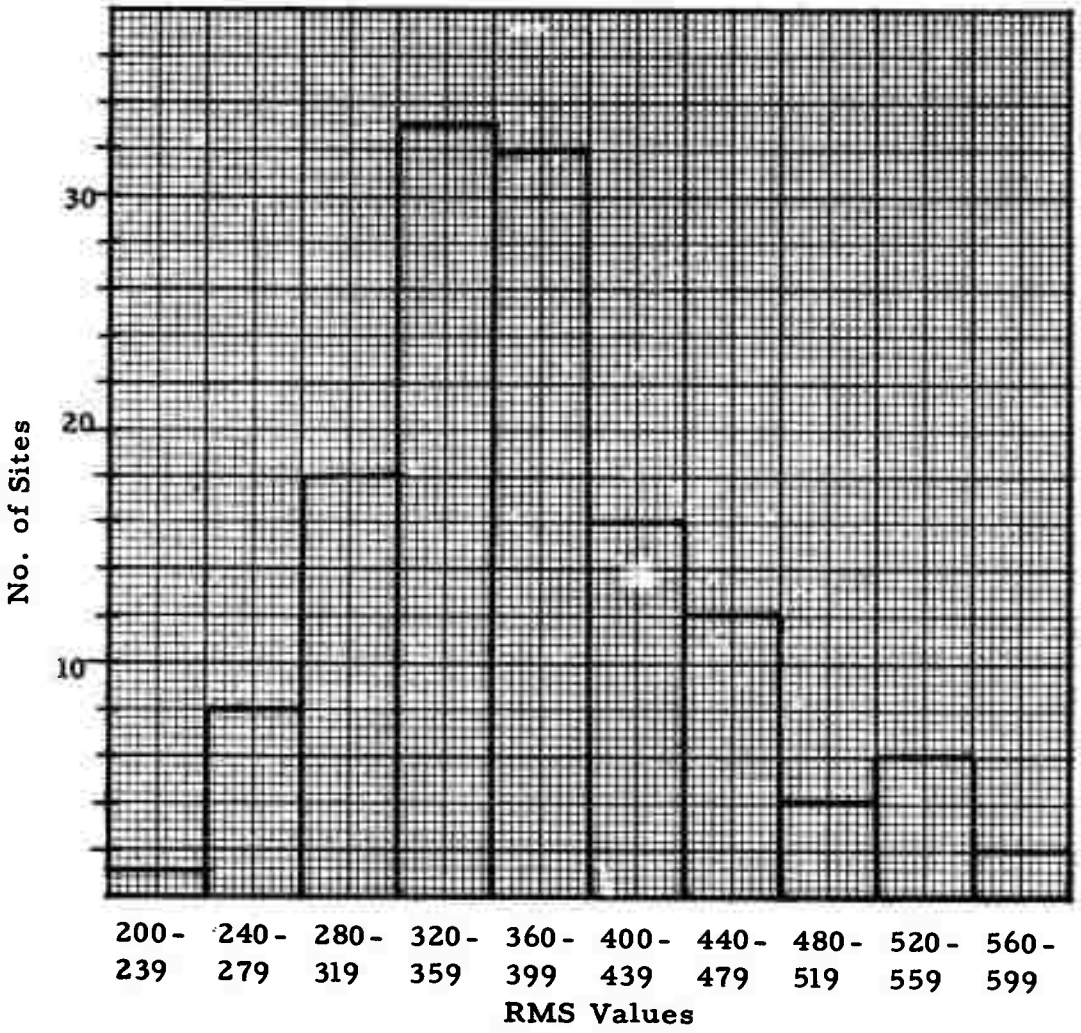


FIGURE V-1

HISTOGRAM FOR NORSAR SHORT PERIOD NOISE RMS LEVELS
GREECE NOISE SAMPLE

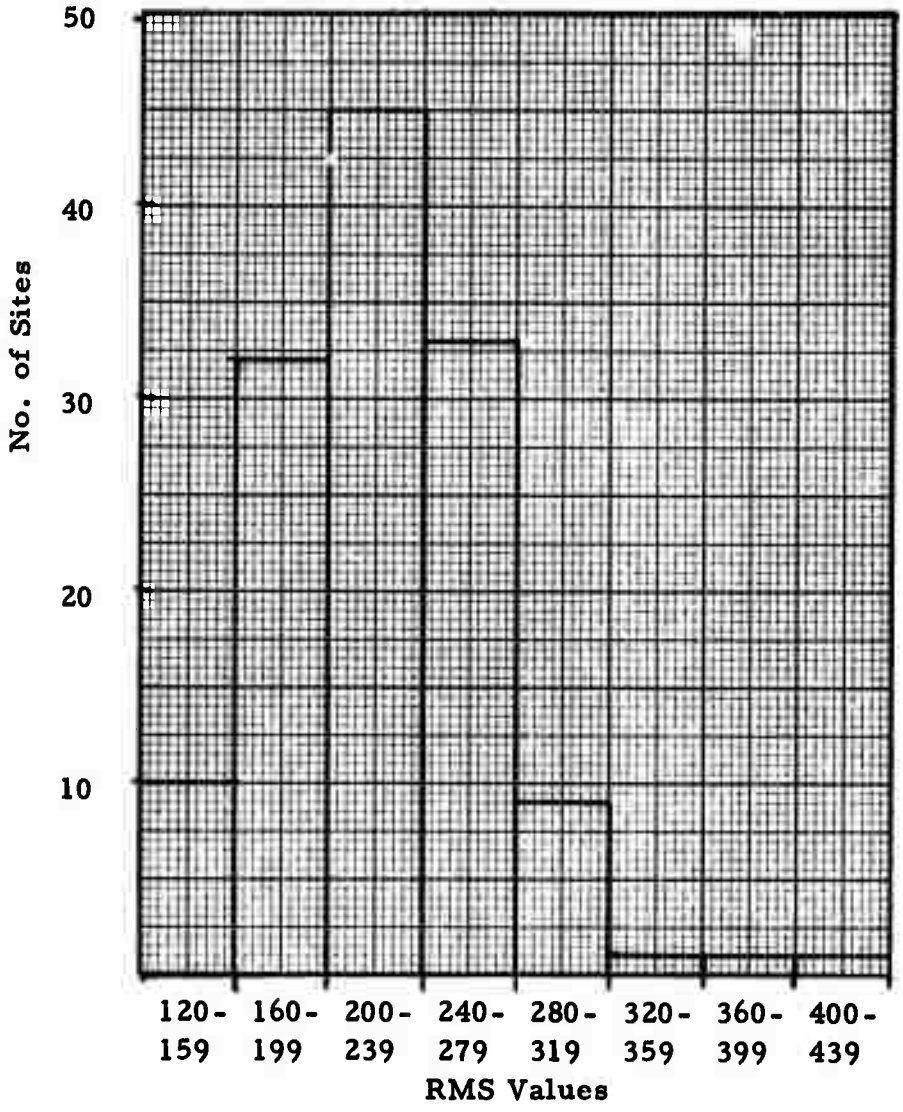


FIGURE V-2

HISTOGRAM FOR NORSAR SHORT PERIOD NOISE RMS LEVELS BEFORE EVENT 11

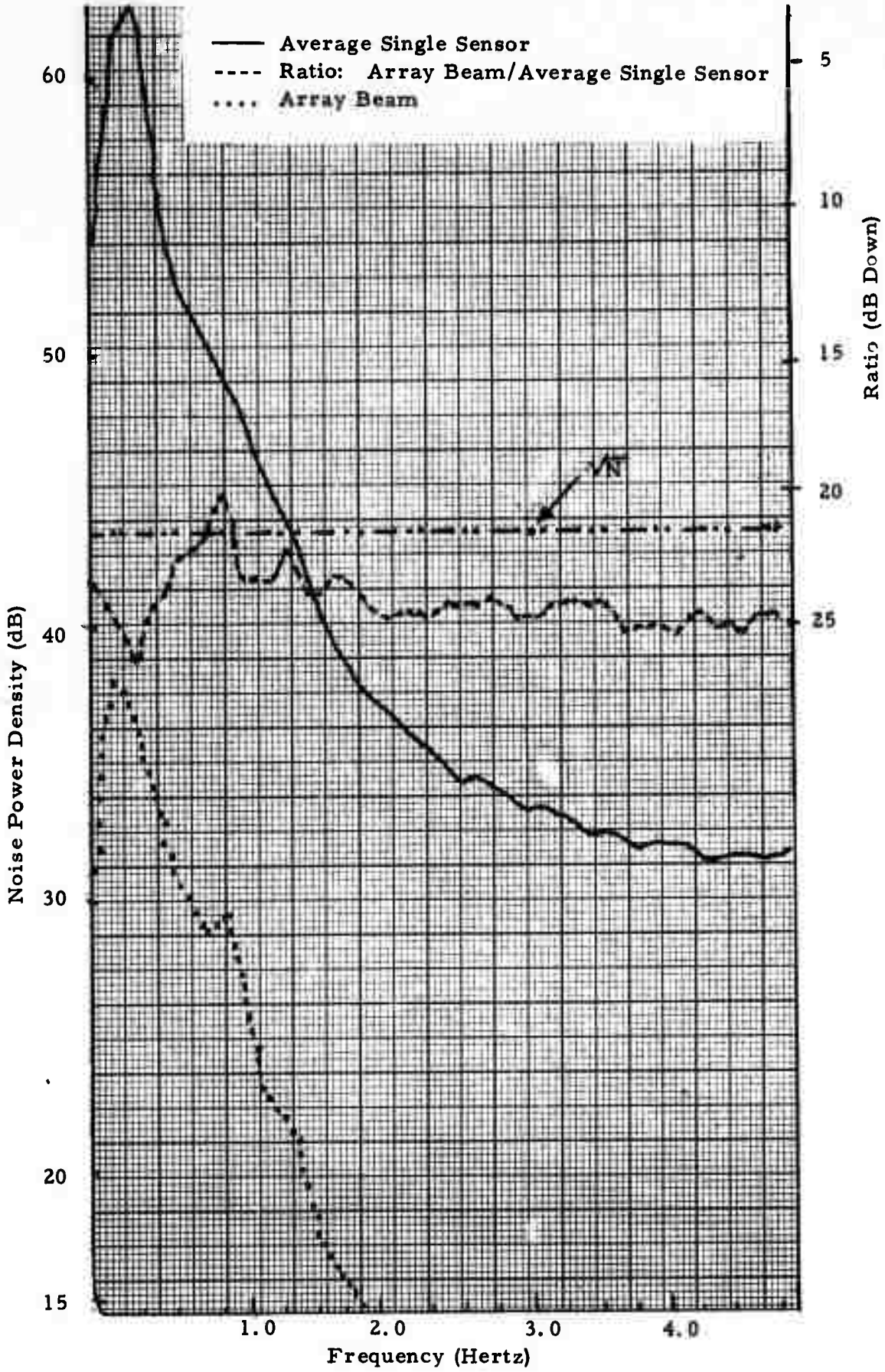


FIGURE V-3

ARRAY BEAM & AVERAGE SINGLE SENSOR NOISE POWER SPECTRA
GREECE NOISE SAMPLES

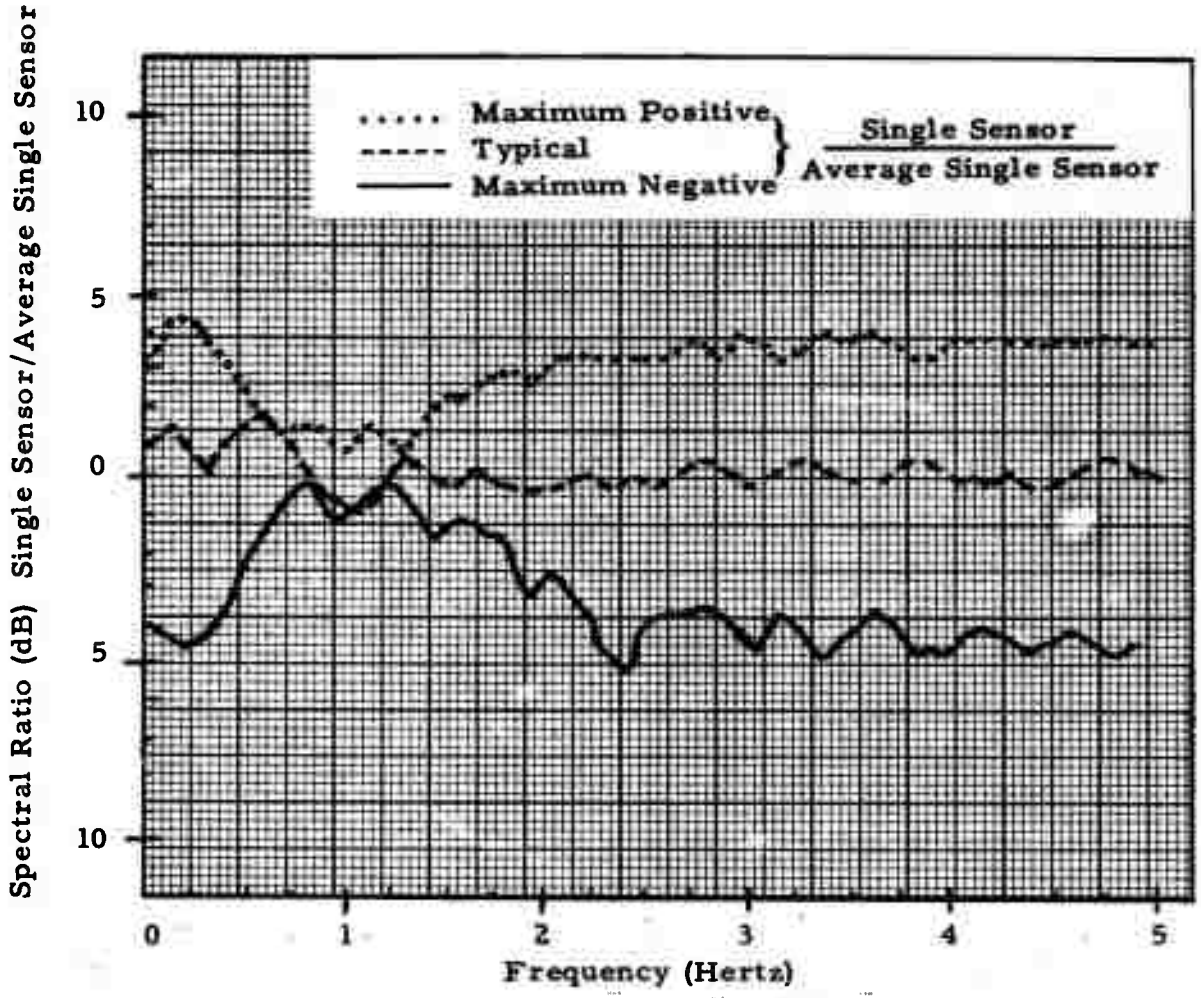


FIGURE V-4
SINGLE SENSOR NOISE SPECTRAL RATIO VARIATIONS
GREECE NOISE SAMPLE

single sensor power spectra are very similar; the maximum positive or negative variation is about 5 dB, and for most sensors it is less than 2 dB at all frequencies.

Only one anomaly was noted in the single sensor power spectra; sensors 0 and 1 of subarray 22 had a spectral line at 2.8 Hz. This anomaly persisted in the remaining 13 noise samples.

Figure V-5 shows the array beam spectrum, the average subarray beam spectrum, and the spectral ratio of the array beam to the average subarray beam for the Greece noise sample. Again, the simple spectral shape of the noise and the $\sqrt{N}$ noise rejection over the entire band is evident.

Variations in the noise spectra of the subarray beams were examined by comparing the ratio of each subarray beam to the average subarray beam. In the region of significant power density (0 to 2.0 Hz) all subarrays were within 2 dB of the average subarray spectrum.

Multiple coherences within a subarray (five sensors on ring predicting the central sensor of the subarray) were calculated for the 22 subarrays. A typical multiple coherency plot (subarray 10) is given in Figure V-6 for the Greece sample. Except for the peak at 3 to 6 seconds, coherence is low at all frequencies where there is significant energy. The 3 to 6 second energy is well below the signal band, and so can be removed by band pass filtering. Above 2 Hz, energy levels are at least 25 dB below the spectral peak, so that there is little energy to remove. The moderate coherence here may possibly be due to the system electronics. In any event it is clear that multichannel processing would not be necessary at the subarray level.

Multiple coheriencies calculated between subarrays were very low, as expected, because of the large distance involved. Figure V-7 shows the multiple coherence between the reference sensor of subarray 1 and the reference sensors of subarrays 2, 3, 4, 6 and 8 for the Greece sample; very low values were obtained.

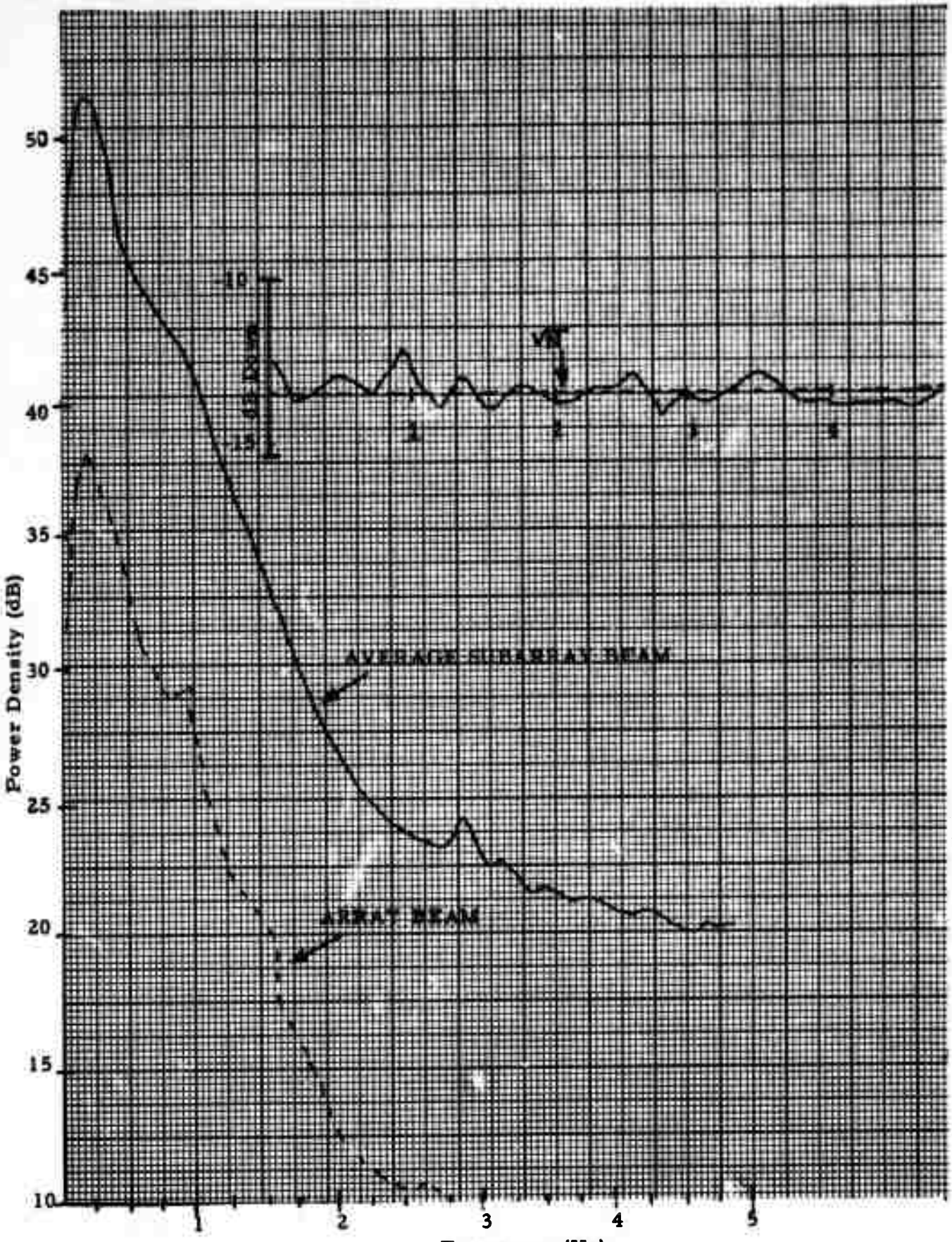


FIGURE V-5

NOISE POWER DENSITY FOR ARRAY AND AVERAGE SUBARRAY BEAMS
GREECE NOISE SAMPLE

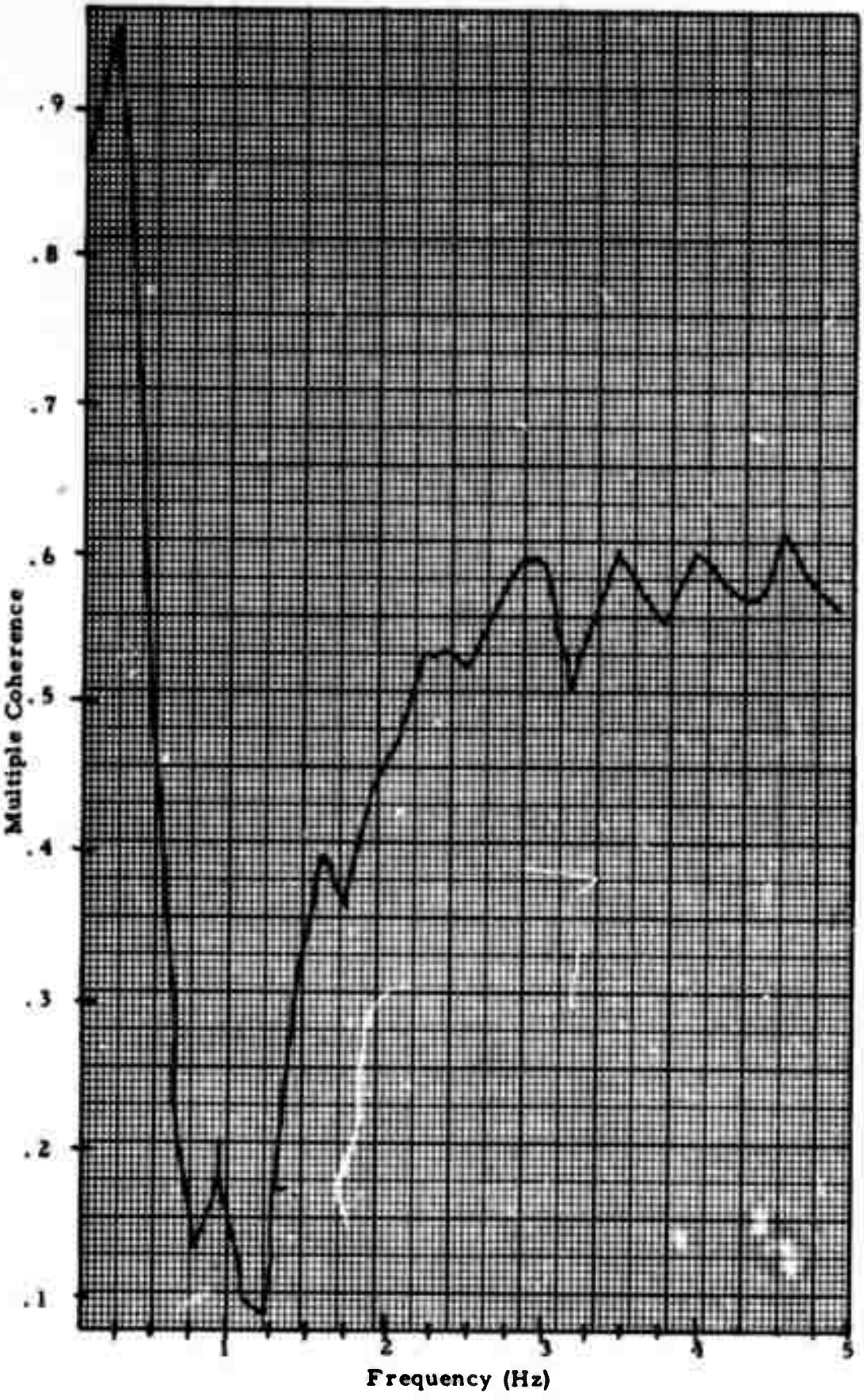


FIGURE V-6
MULTIPLE COHERENCE FOR SUBARRAY 10 NOISE FIELD
GREECE NOISE SAMPLE

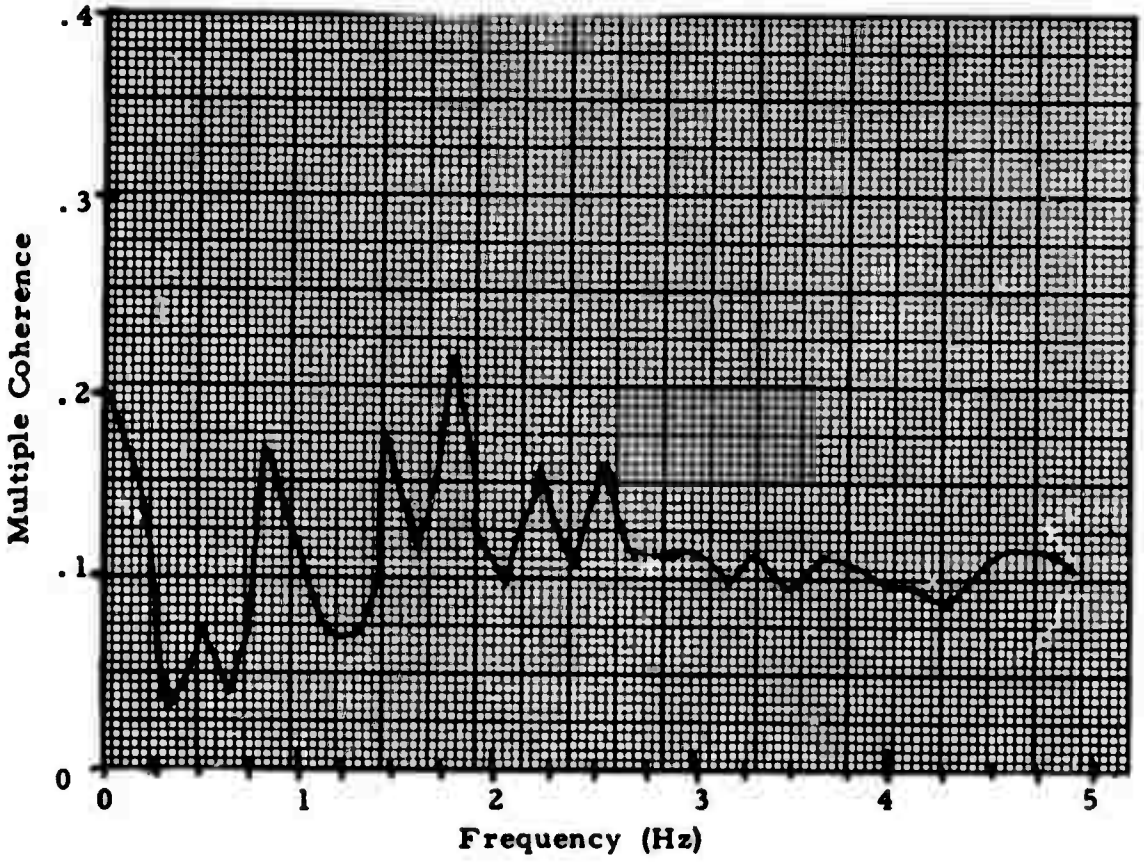


FIGURE V-7

MULTIPLE COHERENCE BETWEEN THE REFERENCE SENSOR OF SUBARRAY 1 AND THE REFERENCE SENSORS OF SUBARRAYS 2, 3, 4, 6 AND 8 GREECE NOISE SAMPLE

Examination of the 13 other noise samples indicates that, with rare exceptions confined to individual subarrays, the noise behaves very much like the noise preceding event 1 from Greece. As expected, however, power levels fluctuate from day to day. Table V-2 gives the RMS level of the array beam for 13 noise samples. The first three characters of each noise sample name correspond to the region of the event which followed. The middle three digits give the Julian date, and the last two digits give the hour. RMS levels are in computer counts. A factor of 3 (10 dB) variability is observed. However there does not appear to be a consistent trend over the two month time period analyzed.

In summary, this preliminary analysis has shown:

- The short period array appears to be operating quite reliably
- The noise spectrum is quite simple, with a peak at 3 to 6 seconds and a very rapid decrease with increasing frequency
- Spectral variability across the array is quite small, less than $\pm$ 2 dB for array beams
- Noise coherence is low, except at the 3 to 6 second peak (which is outside the signal band)
- $\sqrt{N}$ noise rejection is achieved by simple beamforming over the entire signal band.
- Approximately 10 dB variation in broadband noise power was observed in 13 noise samples spread over two months.

C. Signal Analysis

Fifteen signals recorded by the entire NORSAR array (132 sensors) were analyzed in order to study signal characteristics. The following studies were performed for these events:

TABLE V-2

NOISE RMS LEVELS OF ARRAY BEAM

| Event | Name | RMS Level | RMS Level (dB) |
|---|---|---|---|
| 1 | GRE/068/04N | 23.00 | 27.2 |
| 4 | KIR/082/09N | 14.91 | 23.5 |
| 5 | KIR/082/20N | 17.87 | 25.0 |
| 6 | KIR/083/20N | 15.82 | 24.0 |
| 7 | TIB/093/07N | 12.01 | 21.6 |
| 8 | KUR/099/15N | 11.86 | 21.5 |
| 9 | YUG/100/02N | 9.51 | 19.5 |
| 10 | KUR/101/08N | 24.22 | 27.7 |
| 11 | IRA/102/19N | 17.60 | 24.9 |
| 12 | KAZ/108/23N | 23.43 | 27.4 |
| 13 | GRE/109/02N | 28.94 | 29.2 |
| 14 | TAD/110/03N | 24.08 | 27.6 |
| 15 | TIB/123/00N | 11.82 | 21.5 |

- Signal similarity investigations
- Signal spectrum measurements
- Noise and signal spectral comparisons
- Delay-time anomalies (deviation from plane wave propagation)

Qualitative estimates of signal similarity were made by analysis of all sensors for events 1 and 2 and of subarray outputs for all 15 events. Within a subarray, the waveforms were much the same for the entire length of the event. However, between the subarray outputs, there was moderate similarity only for the first few cycles of an event. Significant differences occured within a few seconds after the signal arrival. As a result, array beams formed from the 22 subarray outputs show a moderate power drop compared with the strongest subarray a few seconds after a signal arrival.

Signal amplitude variations between subarray outputs are striking (note that the seismometers appear to be well equalized). For the GRE/068/04N event, the peak-to-peak/2 values are shown in Figure V-8. These values vary from 1999 at subarray 12 to 589 at subarray 6 (10.6 dB variation). For this event, the southwest quadrant of the NORSAR array (subarrays 6, 7, 15, 16, 17, 18, 19, 20, and 21) exhibits peaks below 1000, while the northeast section (subarrays 12, 13, and 14) has peaks above 1500. For the URA/082/06N event, the corresponding zero-to-peak values are shown in Figure V-9. These values vary from 7830 at subarray 11 to 5438 at subarray 7 (3.2 dB variation). Subarray 12 still had the highest signal-to-noise ratio for this event. In the old Plan D events from the Kazakh test site, the signal amplitude variations consistantly exceeded the variations of the GRE/068/04N event. In most of the 15 NDPC events processed, subarrays 11 or 12 were the strongest. However, for the two events from the Kurile Islands region, subarray 3 was the strongest subarray. Since subarray 3 is located on the inner ring of the NORSAR array, it is clear that the location of the strongest subarray is no simple function of event epicenter.

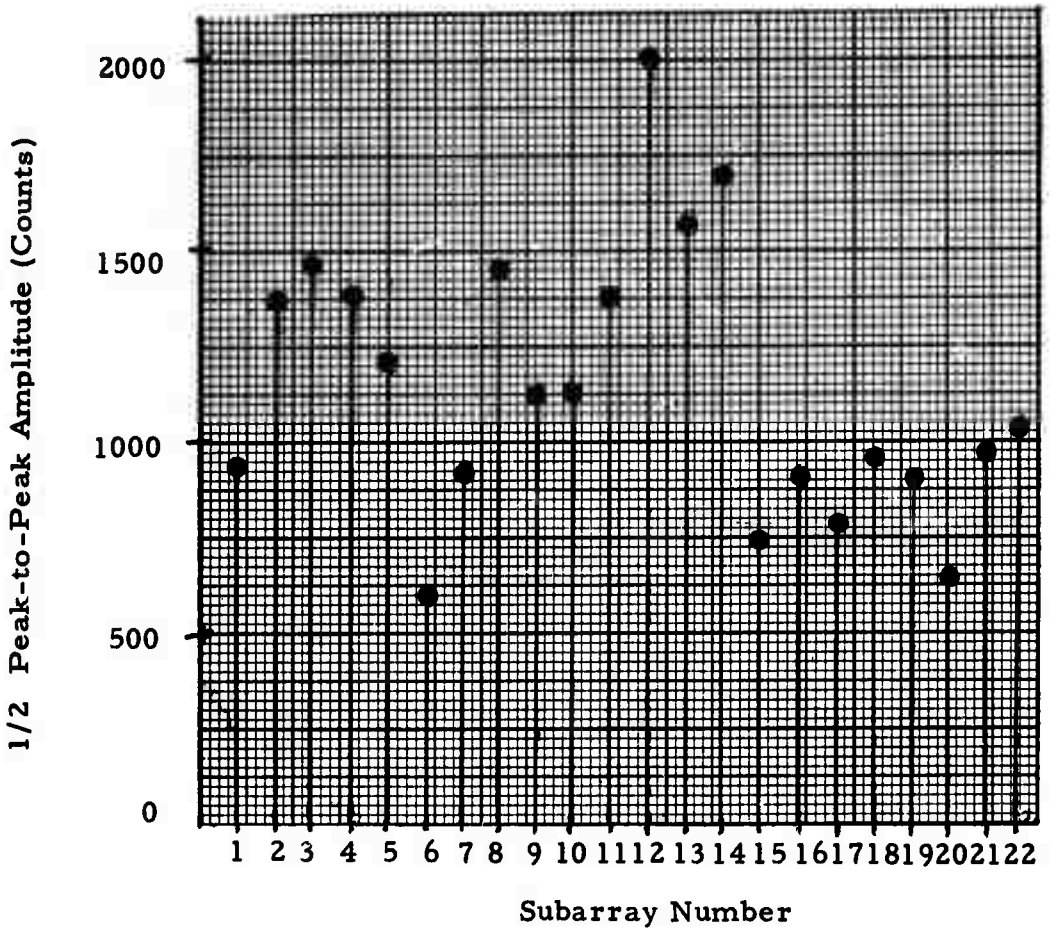


FIGURE V-8

SUBARRAY SIGNAL AMPLITUDES FOR GRE/068/04N

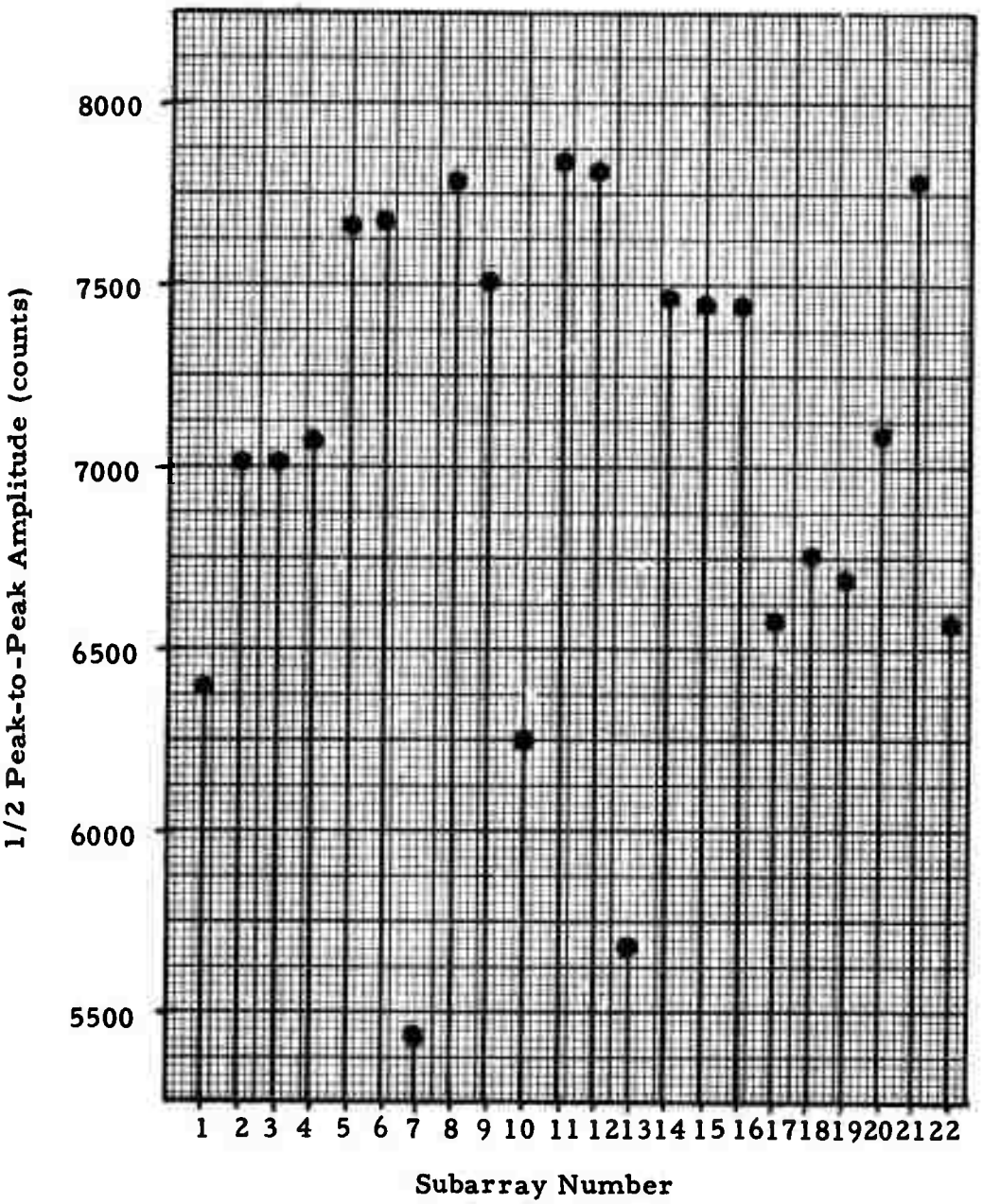


FIGURE V-9
SUBARRAY SIGNAL AMPLITUDES FOR URA/082/06N

The signal spectral characteristics for the GRE/068/04N event were examined using the subarray 12 beam, which had the largest signal-to-noise ratio. The subarray 12 signal plus noise spectrum for the 128-second gate is shown in Figure V-10; the noise spectrum for 320-second gate just preceding the signal also is plotted for reference. The signal energy is concentrated in a band from 0.5 to 1.5 Hz with a sharp drop in power density on either side of this band. The signal-to-noise ratio is best between 1.0 and 1.5 Hz, suggesting that signal detection may best be accomplished at NORSAR at relatively high frequencies.

Figure V-11 shows the effect of plane-wave beamforming on signal strength for the GRE/068/04N event. The average single sensor spectrum, the average subarray beam spectrum (using plane wave delays) and the array beam (also using plane wave delays) are shown; a 128-second signal gate was used to obtain the spectral estimates. The corresponding noise spectra computed from a 320-second signal gate just preceding the signal were shown previously; note that the signal-to-noise ratio for this event is only fair.

At the 1.0 Hz signal peak, signal loss resulting from subarray beamforming is 2 dB; this is slightly higher than expected. However, the low signal-to-noise ratio at several of the subarrays could account for part of the loss. It appears that plane wave delays are adequate for forming subarray beams, as is the case at LASA (Harley, 1967).

Plane wave delays clearly are inadequate for array beamforming. Signal loss at 1.0 Hz is 9 dB (relative to the average subarray beam) and the array beam signal-to-noise ratio is not much better than that for the average subarray beam (and in fact significantly worse than that for certain high-amplitude subarrays). Thus time delay anomaly corrections are essential for successful array beamforming; this is discussed in more detail in the next section.

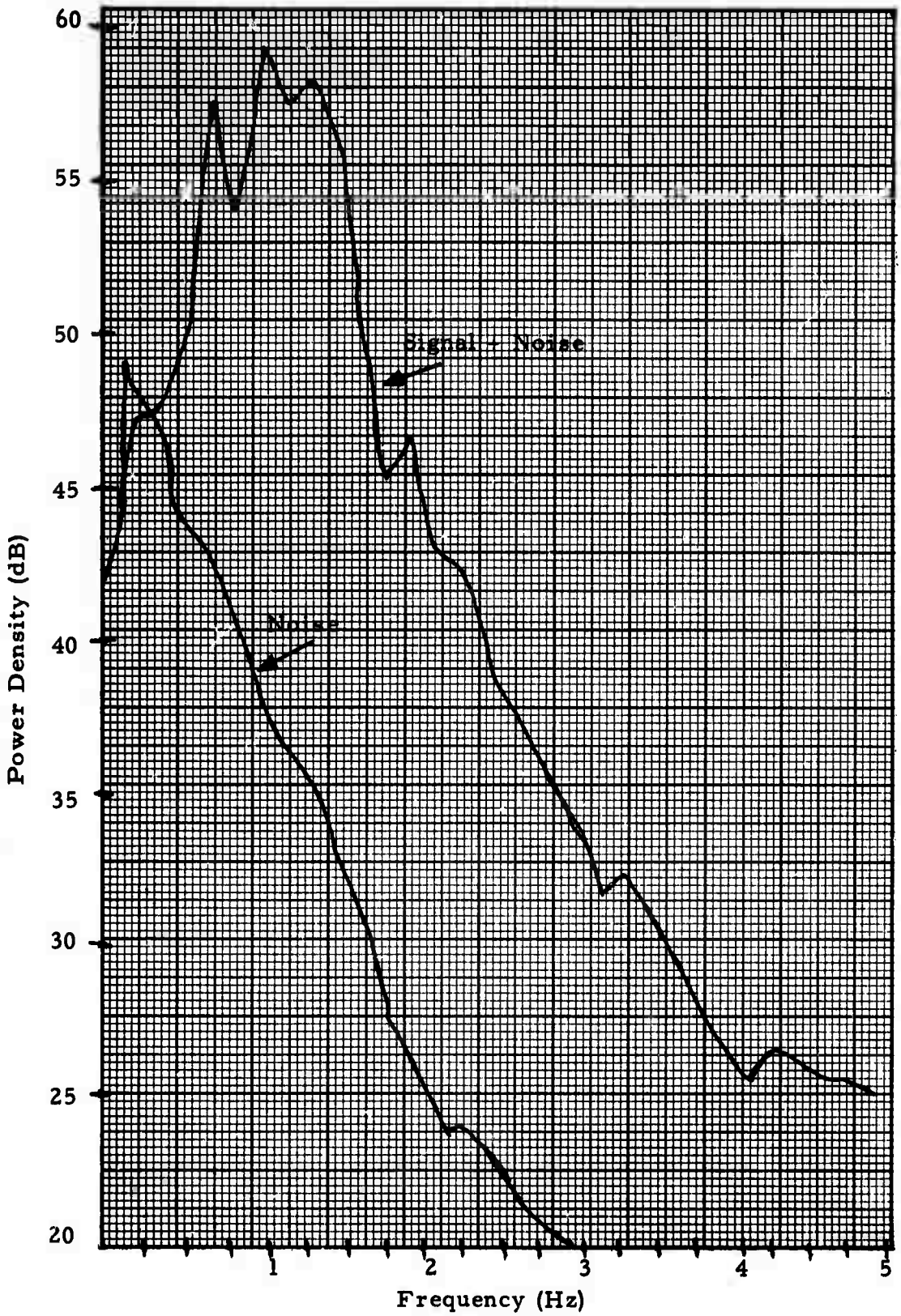


FIGURE V-10
SUBARRAY 12 SIGNAL SPECTRUM FOR GRE/068/04N

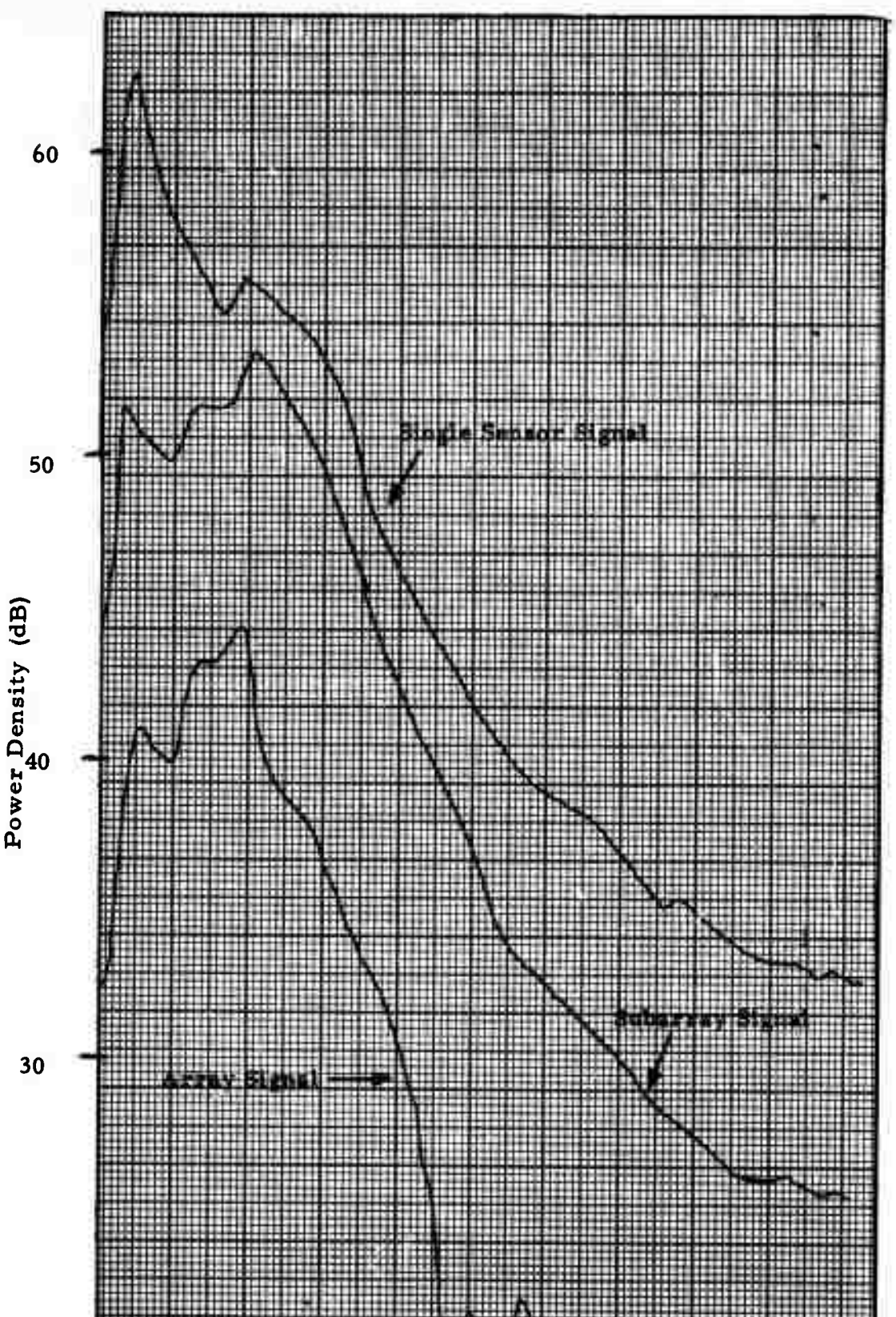


FIGURE V-11

SIGNAL AND NOISE SPECTRA FOR AVERAGE SINGLE SENSOR, AVERAGE SUBARRAY BEAM, AND PLANE WAVE ARRAY BEAM FOR GRE/068/04N

Figure V-12 shows a spectrum for the first 6.4 seconds after the arrival of URA/082/06N and represents the power density for the output of a diversity-stack beam. The bodywave magnitude for this event is 5.6, and the signal-to-noise ratio is very large. In comparison with the other 14 events, the spectrum is relatively uniform from 0.5 Hz to beyond 2.0 Hz, where it begins its final falloff. A comparison with typical noise spectra shows that the highest signal-to-noise ratio for this event occurs around 2.0 Hz.

Figure V-13 shows a spectrum for the first 12.8 seconds after the arrival of KIR/082/20N on a diversity-stack beam. The event bodywave magnitude is 6.0, and the signal-to-noise ratio is very large. The spectral values below 0.5 Hz represent power density after application of a 0.5-5.0 Hz bandpass filter. This spectrum is typical of all events except the Ural Mountains event just discussed. In the Kirgiz event, the spectrum tends to fall off beginning at 1 Hz. The highest signal-to-noise ratio for this event occurs around 1.5 Hz.

In summary, this preliminary signal analysis has shown:

- Signal similarity appears to be fairly good within a subarray, and reasonably good in the first few cycles of the signal between subarrays.
- Signal amplitude variations across the array are significant
- For all but the Ural Mountains event, signal-to-noise ratios were highest between 1.0 and 1.5 Hz. For that event, the signal-to-noise ratio was highest at about 2.0 Hz.
- Theoretical plane wave delays appear to be adequate for subarray beamforming, but time delay anomaly corrections are required for array beamforming.

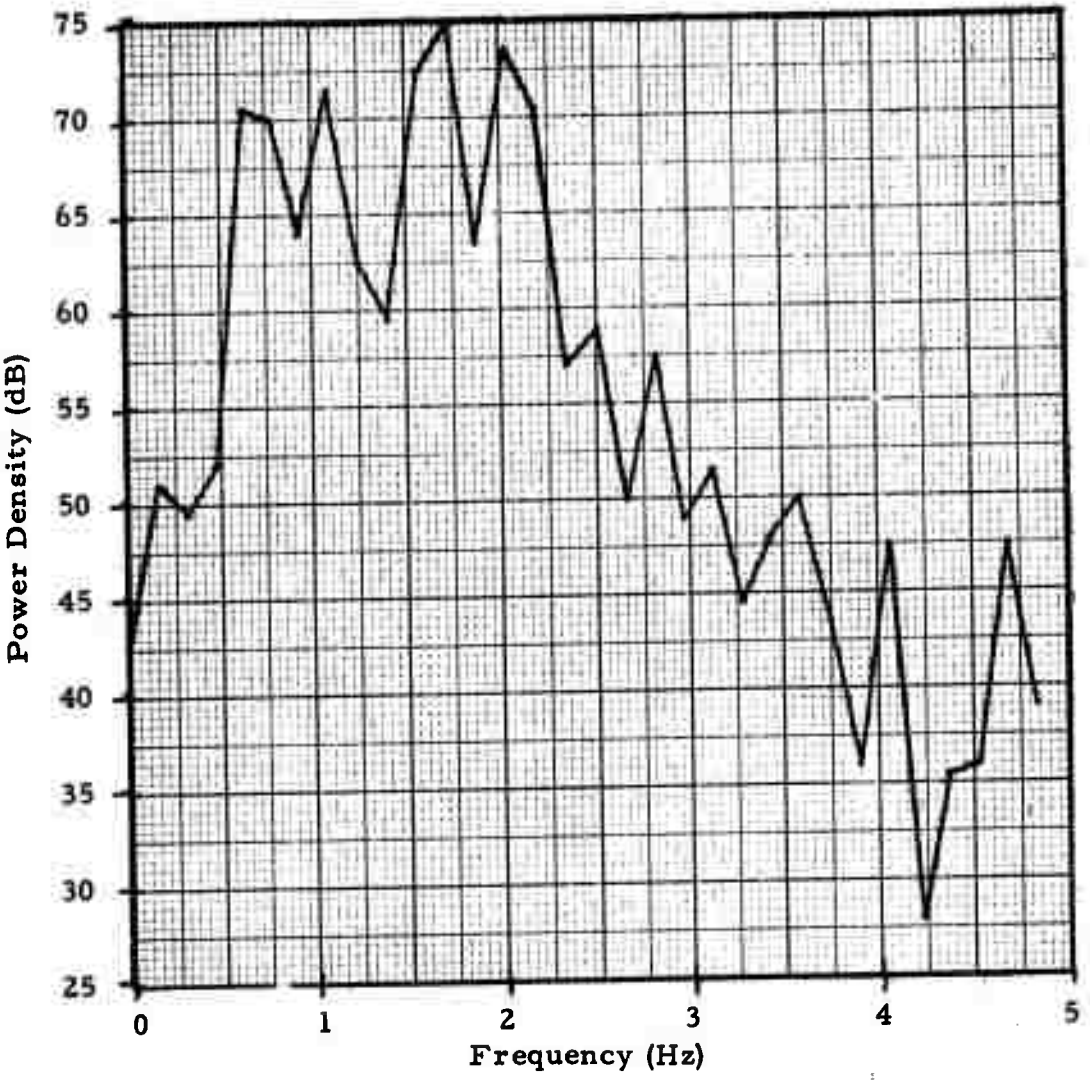


FIGURE V-12

DIVERSITY-STACK SIGNAL SPECTRUM FOR 6.4 SECONDS AFTER ARRIVAL OF URA/082/06N

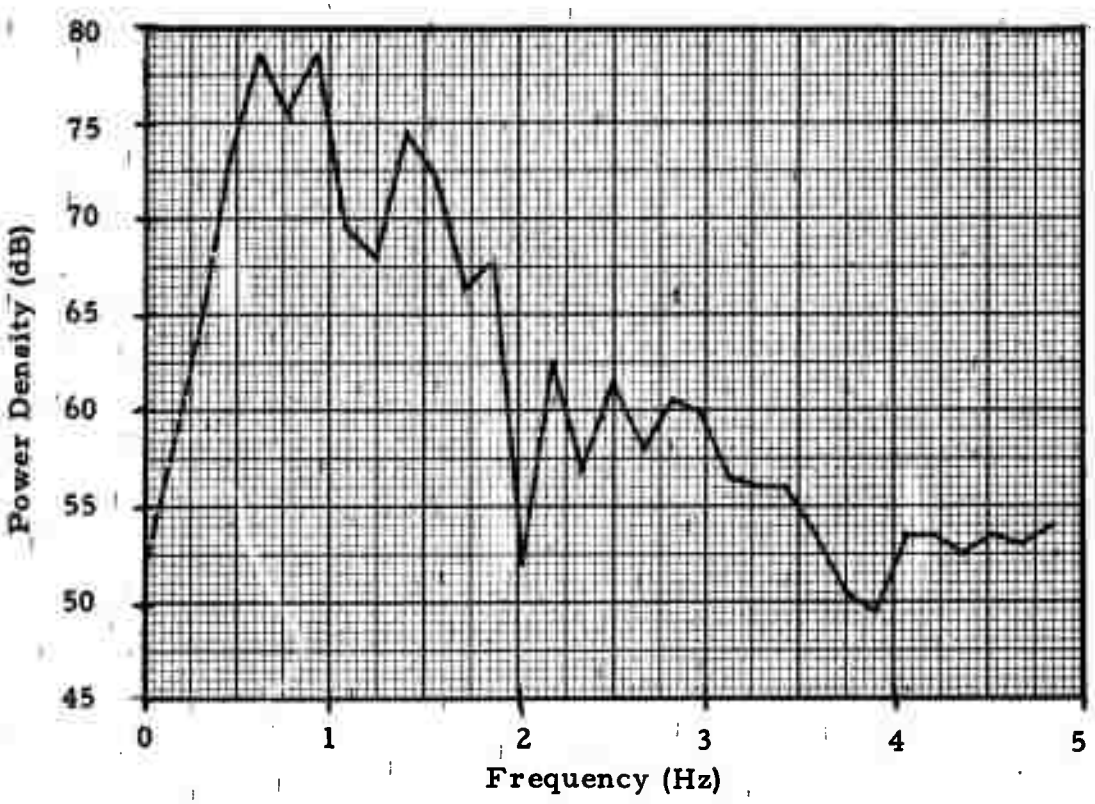


FIGURE V-13

DIVERSITY-STACK SIGNAL SPECTRUM FOR 12.8 SECONDS AFTER ARRIVAL OF KIR/082/20N

## D. Array Beamforming Results

As mentioned in the previous subsection, there were two principal problems encountered in forming beams to enhance signals propagating across the NORSAR array. First, the wavefront arrival time at the individual subarrays were not consistent with plane wave propagation at the expected velocity and azimuth. Second, large variations in the received signal amplitude occurred between subarrays.

In an attempt to remove the inter-subarray delay anomalies, cross-correlation functions were computed between a reference subarray beam and the remaining subarray beams in order to obtain an adusted set of delays. The reference subarray generally was chosen to be the one with the highest signal-to-noise ratio. This method worked well when the subarrays had high signal-to-noise ratios, but for the subarrays with the weakest signals, results were unsatisfactory. For these subarrays, delays were obtained by a combination of visual inspection, examination of crosscorrelation functions, and comparison of delay anomalies from other nearby events.

After removing the delay anomalies, the subarrays were weighted to give a diversity-stack beam. In this technique, each subarray is weighted proportionate to the subarray signal-amplitude to noise-power ratio and added to the other weighted and shifted subarray traces. A detailed study of a five-minute noise sample just before GRE/068/04N event showed that it was necessary to use noise gates up to 60 seconds in length before the power variations with time were reduced to the same level as the variations in power between the subarray outputs over the entire five-minute noise sample. Based on the noise analysis results shown previously the assumption of equal noise power on all subarray beams is quite reasonable. All subarray outputs were therefore assumed to have the same noise power. The signal amplitude for each subarray was computed

using the RMS level over a 6.4-second or 12.8-second window beginning with the signal arrival.

Beams were formed in this way for six of the 15 signals successfully edited. Results for these events are shown in Table V-3 in terms of the resulting signal-to-noise ratios for the reference subarray, the plane-wave beam, the adjusted-delay beam, and the diversity-stack beam. Noise power was computed over a 70-second gate preceding the signal. Signal power was computed over a 6.4-second or 12.8-second window beginning with the signal arrival. The reference subarray used was always the subarray with the highest signal-to-noise ratio. A common set of adjusted delays was applied to the three Kirgiz-Sinkiang border events.

Improvement in the diversity-stack beams ranged from 2.9 to 8.1 dB relative to the reference subarray, from 1.7 to 9.3 dB relative to the plane-wave beam, and from -0.1 to 2.3 dB relative to the adjusted-delay beam. Most of the improvement is obtained from application of the adjusted delays. In only one case did the improvement over the adjusted-delay beam exceed 0.7 dB. The usefullness of the diversity-stack technique will require additional analysis. In particular, a small ensemble of events from Eastern Kazakh will be used for evaluation. The old "Plan D" data indicated that signal amplitude variations were largest for this location, and hence the diversity-stack technique would be expected to give the largest improvement over conventional beamsteering.

Plane-wave and adjusted delays for Eastern Kazakh, Alma-Ata, and the GRE/068/04N event are shown in Table V-4. The Eastern Kazakh and Alma-Ata delays were obtained from "Plan D" data recorded in 1970. The Greece event had only a moderate signal-to-noise ratio, so that the tabulated delay anomalies are less certain than for the other events. Delay anomalies of 0.5 seconds were typical; note that an anomaly of this size is enough to cause half-cycle errors in the time alignment of 1 Hz signals (and hence cancellation).

TABLE V-3

BEAM SIGNAL-TO-NOISE RATIOS FOR SIX EVENTS

| Event | Bandpass (Hz) | $m_b$ | Signal-to-Noise Ratio (dB) | | | |
|---|---|---|---|---|---|---|
| | | | Reference Subarray | Plane-Wave Beam | Adjusted-Delay Beam | Diversity Stack Beam |
| URA/082/06N | 0.05-5.0 | 5.6 | 38.4 | 39.3 | 43.1 | 43.6 |
| KIR/082/09N | 0.5-5.0 | 5.7 | 38.2 | 37.0 | 40.8 | 41.1 |
| KIR/082/20N | 0.5-5.0 | 6.0 | 32.4 | 36.7 | 38.5 | 38.4 |
| KIR/083/20N | 0.5-5.0 | 5.3 | 30.1 | 30.2 | 35.8 | 36.5 |
| TIB/093/07N | 0.5-5.0 | 5.1 | 6.3 | 6.1 | 14.1 | 14.4 |
| YUG/100/02N | 0.5-5.0 | 4.6 | 18.6 | 13.1 | 20.0 | 22.4 |

using the RMS level over a 6.4-second or 12.8-second window beginning with the signal arrival.

Beams were formed in this way for six of the 15 signals successfully edited. Results for these events are shown in Table V-3 in terms of the resulting signal-to-noise ratios for the reference subarray, the plane-wave beam, the adjusted-delay beam, and the diversity-stack beam. Noise power was computed over a 70-second gate preceding the signal. Signal power was computed over a 6.4-second or 12.8-second window beginning with the signal arrival. The reference subarray used was always the subarray with the highest signal-to-noise ratio. A common set of adjusted delays was applied to the three Kirgiz-Sinkiang border events.

Improvement in the diversity-stack beams ranged from 2.9 to 8.1 dB relative to the reference subarray, from 1.7 to 9.3 dB relative to the plane-wave beam, and from -0.1 to 2.3 dB relative to the adjusted-delay beam. Most of the improvement is obtained from application of the adjusted delays. In only one case did the improvement over the adjusted-delay beam exceed 0.7 dB. The usefullness of the diversity-stack technique will require additional analysis. In particular, a small ensemble of events from Eastern Kazakh will be used for evaluation. The old "Plan D" data indicated that signal amplitude variations were largest for this location, and hence the diversity-stack technique would be expected to give the largest improvement over conventional beamsteering.

Plane-wave and adjusted delays for Eastern Kazakh, Alma-Ata, and the GRE/068/04N event are shown in Table V-4. The Eastern Kazakh and Alma-Ata delays were obtained from "Plan D" data recorded in 1970. The Greece event had only a moderate signal-to-noise ratio, so that the tabulated delay anomalies are less certain than for the other events. Delay anomalies of 0.5 seconds were typical; note that an anomaly of this size is enough to cause half-cycle errors in the time alignment of 1 Hz signals (and hence cancellation).

TABLE V-4

NORSAR SHORT-PERIOD DELAYS AND DELAY ANOMALIES FOR 3 REGIONS

(desiseconds)

| | KAZAKH AREA (50.0N, 78.0E) | | | ALMA-ATA EVENT (42.5N, 78.8E) | | | GREECE EVENT (38.7N, 20.3E) | | |
|---|---|---|---|---|---|---|---|---|---|
| Subarray | Adjusted Delay | Plane-Wave Delay | Dev. | Adjusted Delay | Plane-Wave Delay | Dev. | Adjusted Delay | Plane-Wave Delay | Dev. |
| 1 | | | | | | | 7 | 11 | -4 |
| 2 | -34 | -38 | 4 | -33 | -38 | 5 | -14 | -11 | -3 |
| 3 | -19 | -21 | 2 | -18 | -20 | 2 | -7 | -4 | -3 |
| 4 | | | | | | | 6 | 9 | -3 |
| 5 | | | | | | | 22 | 31 | -9 |
| 6 | -39 | -44 | 5 | -33 | -39 | 6 | 22 | 31 | -9 |
| 7 | | | | | | | 7 | 14 | -7 |
| 8 | -49 | -53 | 4 | -46 | -51 | 5 | -10 | -5 | -5 |
| 9 | -37 | -39 | 2 | -40 | -42 | 2 | -49 | -44 | -5 |
| 10 | -29 | -31 | 2 | -31 | -33 | 2 | -40 | -34 | -6 |
| 11 | -9 | -8 | -1 | -11 | -10 | -1 | -24 | -23 | -1 |
| 12 | 0 | 0 | 0 | 0 | 0 | 0 | 0 | 0 | 0 |
| 13 | 2 | 1 | 1 | 3 | 2 | 1 | 15 | 14 | 1 |
| 14 | -14 | -17 | 3 | -10 | -13 | 3 | 24 | 29 | -5 |
| 15 | -16 | -21 | 5 | -9 | -15 | 6 | 59 | 58 | 1 |
| 16 | -31 | -37 | 6 | -24 | -31 | 7 | 48 | 49 | -1 |
| 17 | -51 | -58 | 7 | -45 | -51 | 6 | 46 | 48 | -2 |
| 18 | -65 | -69 | 4 | -59 | -62 | 3 | 38 | 37 | 1 |
| 19 | -65 | -68 | 3 | -60 | -63 | 3 | 23 | 21 | 2 |
| 20 | -73 | -75 | 2 | -71 | -72 | 1 | 1 | 1 | 0 |
| 21 | -71 | -73 | 2 | -70 | -72 | 2 | -34 | -28 | -6 |
| 22 | -51 | -54 | 3 | -51 | -56 | 5 | -37 | -34 | -3 |

The close agreement between the delay anomalies for the Kazakh area and the Alma-Ata event (separated by 7.5 degrees in latitude and 0.6 degrees in longitude) indicates that a single set of time delay corrections may be useful for a relatively large region. Delay anomalies obtained for the events taken from the NORWAY NDPC tapes tend to confirm the fact that the delay anomalies change relatively slowly as a function of event epicenter. The delay anomalies for the GRE/068/04N event, for example, were useful in deciding the delay anomalies for the GRE/109/02N and YUG/100/02N events.

Figure V-14 shows the URA/082/06N event and illustrates the improvement in signal-to-noise ratio resulting from time delay corrections and the diversity-stack technique. The top trace is the plane-wave beam, the second trace is the adjusted-delay beam, the third trace is the diversity-stack beam, and the fourth trace is subarray 12, the reference subarray. All traces have been filtered to pass the band 0.05 to 5.0 Hz. The traces have been scaled so that, if all subarray outputs sum in phase, the resulting beams would have identical ampltudes.

Due to the fact that the delays used in the plane-wave beam are inaccurate, waveform distortion and signal attenuation are evident in the top wave beam relative to the reference subarray shown in the bottom trace. Use of the adjusted delays, however, produced a significant 4 dB improvement in the adjusted-delay and diversity-stack beams relative to the plane-wave beam. Because of the lack of signal similarity after the first seconds of the signal, the two middle traces show a marked power drop as compared with the reference subarray at the bottom.

## E. Future Plans

During the third quarter of this contract, routine processing of events will continue. In addition, events processed will be run through the Texas Instruments discrimination subroutine.

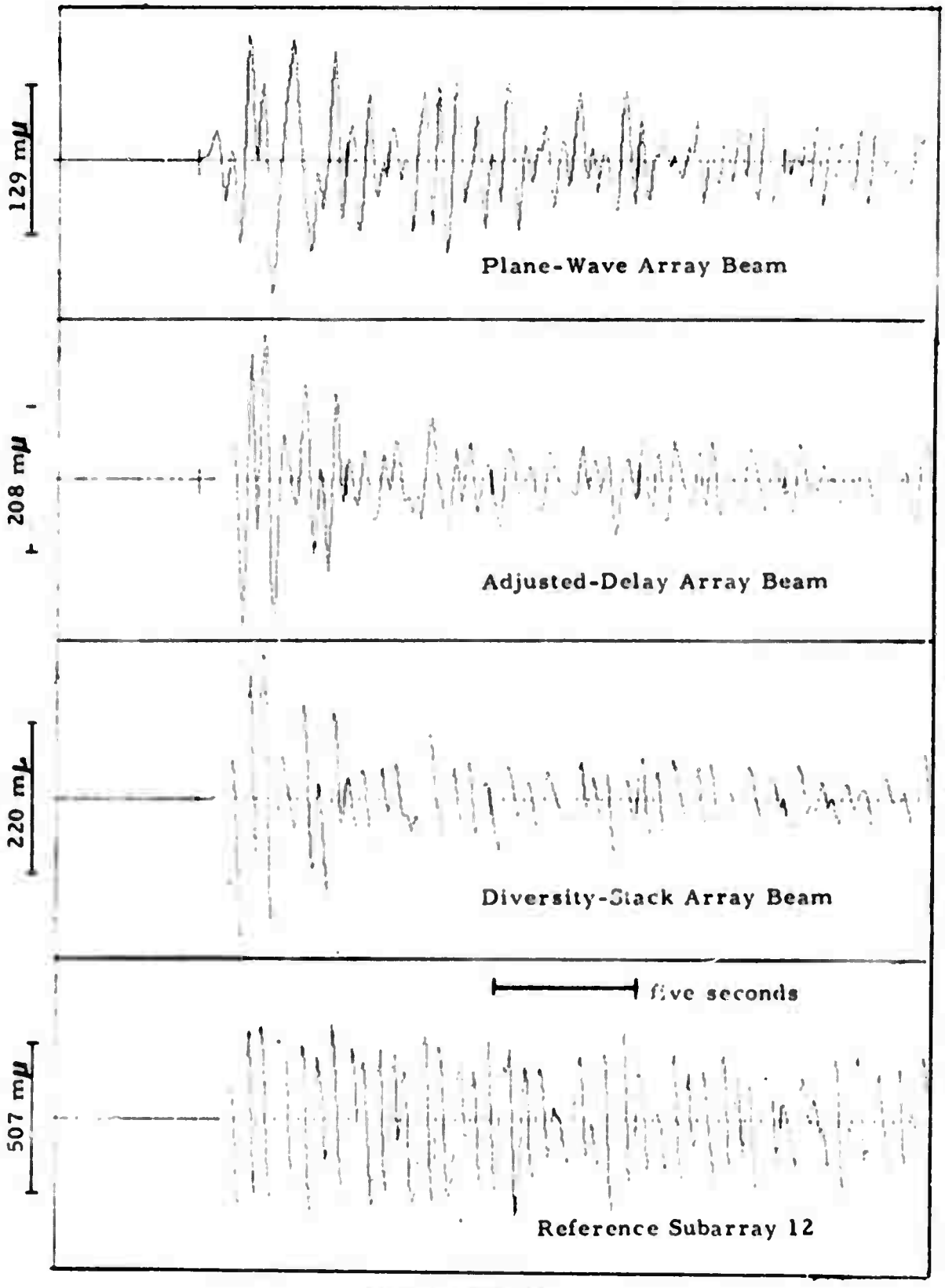


FIGURE V-14

URAL MOUNTAINS EVENT

# VI. LONG PERIOD EXPERIMENT

## A. Introduction

This section describes the work performed during the past quarter on the Long Period Experiment (LPE). The overall objectives of our LPE evaluation are to determine the single station and multistation detection threshold and to determine the multistation discrimination capability. To date the evaluation has been limited by the quality and quantity of the data received at SAAC. This limitation was a result of problems with unreliable station power supplies, component polarity reversals, and unequalized seismometer responses. However, Lamont recently has sent several crews to the stations to correct these problems, and it is expected that better data should be available in the near future from the first five LPE stations. (Note that data recently was received from three of the stations after the modification period). Table VI-1 lists all data received at SAAC.

Because of the problems outlined above, only limited amounts of data were processed during the quarter. The times processed cover the periods January 24, 1971 to February 6, 1971 for stations (sites) 1, 2, 3, 5, 7 (Table VI-2) and February 9, 1971 to March 15, 1971 for station 3. This section describes the results obtained from analyzing these time periods. Included are an analysis of the spectral content and time variability of the noise field at each station, a very preliminary discussion of the detection capability of each station and the network, and the behavior of the $M_s$-$m_b$ classification parameter.

## B. Noise Analysis

The noise analysis discussed in this section covers data from the time period January 24, 1971 to February 6, 1971. Data is presented for the five stations in Table VI-2. It should be noted that data discussed in this section was not of the highest quality, and that it does not represent the current recording capability of the stations. Therefore, these results may not be representative of the current noise field.

TABLE VI-1

LPE DATA RECEIVED AT SAAC FROM LAMONT GEOLOGICAL OBSERVATORY

All days are Julian (Only data from 1971 is shown)

| AUSTRALIA | THAILAND | ALASKA | ISRAEL | OGDENSBURG |
|---|---|---|---|---|
| 1-5 | 23-45 | 1-9 | 1-4 | 1-37 |
| 7-110 | 79-155 | 21-109 | 7-55 | 42-260 |
| 187-255 | | 220-236 | | |

TABLE VI-2

STATIONS OF THE LPE NETWORK

| Station | Code | Coordinates | | Elevation (ft) |
|---|---|---|---|---|
| | | Latitude (deg:min:sec) | Longitude (deg:min:sec) | |
| Australia | 1 | 20:05:18 S | 146:15:16 E | 1168 |
| Thailand | 2 | 18:47:24 N | 98:57:37 E | 1352 |
| Alaska | 3 | 64:53:58 N | 148:00:20 W | 1000 |
| Israel | 5 | 29:19:48 N | 34:32:12 E | 655 |
| Ogdensburg | 7 | 41:04:00 N | 74:37:00 W | -1221 |

1. Spectral Content

To study the spectral content of the noise, a one-hour noise sample from each day of the time period was edited. However, since visual records of the data were not available when the sample time periods were chosen, several of the samples contain unwanted signals. The time periods containing signals or questionable data are not included in the noise analysis. Also, as will be seen in the figures of this and the signal analysis section, none of the stations was operative throughout the entire 14 days of interest.

Figure VI-1 shows noise power density spectra for two days. These spectra have been corrected to millimicrons of ground motion using calibration information furnished by Lamont Observatory. (The corrections are relative to $1(m\mu)^2$/Hz at 0.025 Hz). In the figure only the vertical components have been presented to show the relative noise power at each of the stations. This figure is typical of the spectra for the time period studied and exhibits certain properties of the five noise fields which are discussed below.

The noise fields for sites 2 and 3 are dominated by a large peak at the very long periods. This peak is present on all of the spectra analyzed for the two sites. Site 1 also contains a long period peak for all but one of the samples; however, it is not as dominant as the peak for sites 2 and 3. Site 7 contains a long period peak on less than half of the samples analyzed; note that in the two spectra shown, site 7 has an extremely large peak in the bottom spectra, but the top spectra is relatively flat out to 0.07 Hz. Also, site 5 does not contain a long period peak in any of the samples analyzed; however, the data for this site were limited to the time period Janaury 24, 1971 to January 29, 1971.

For typical long period noise fields the systems were designed so that the noise spectra, as seen through the systems, will be flat in the 20-50 second range. This property was observed in some of the spectra for sites 5 and7. (Figure VI-2)

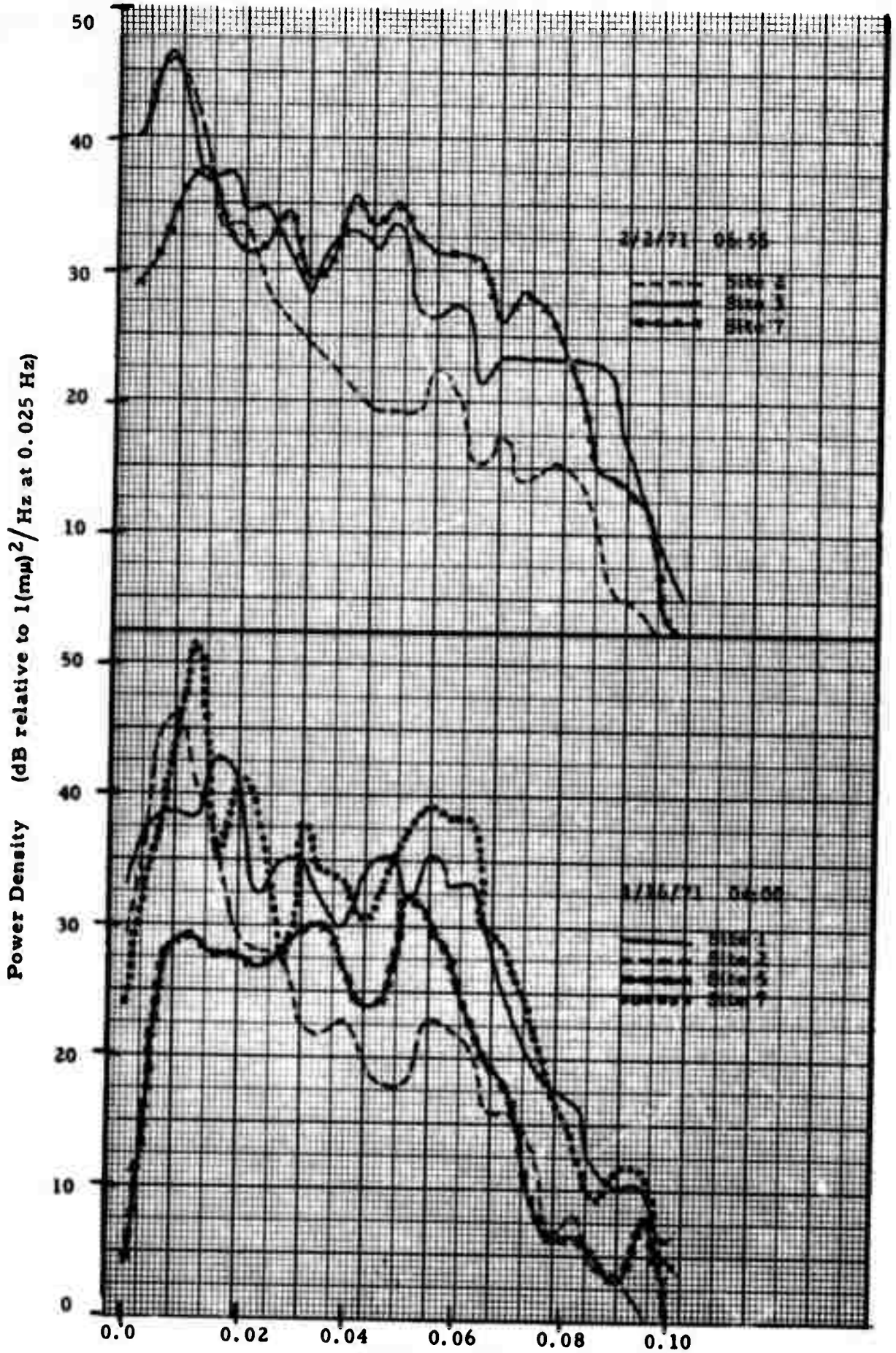


FIGURE VI-1
NOISE POWER DENSITY SPECTRA
(vertical components only)

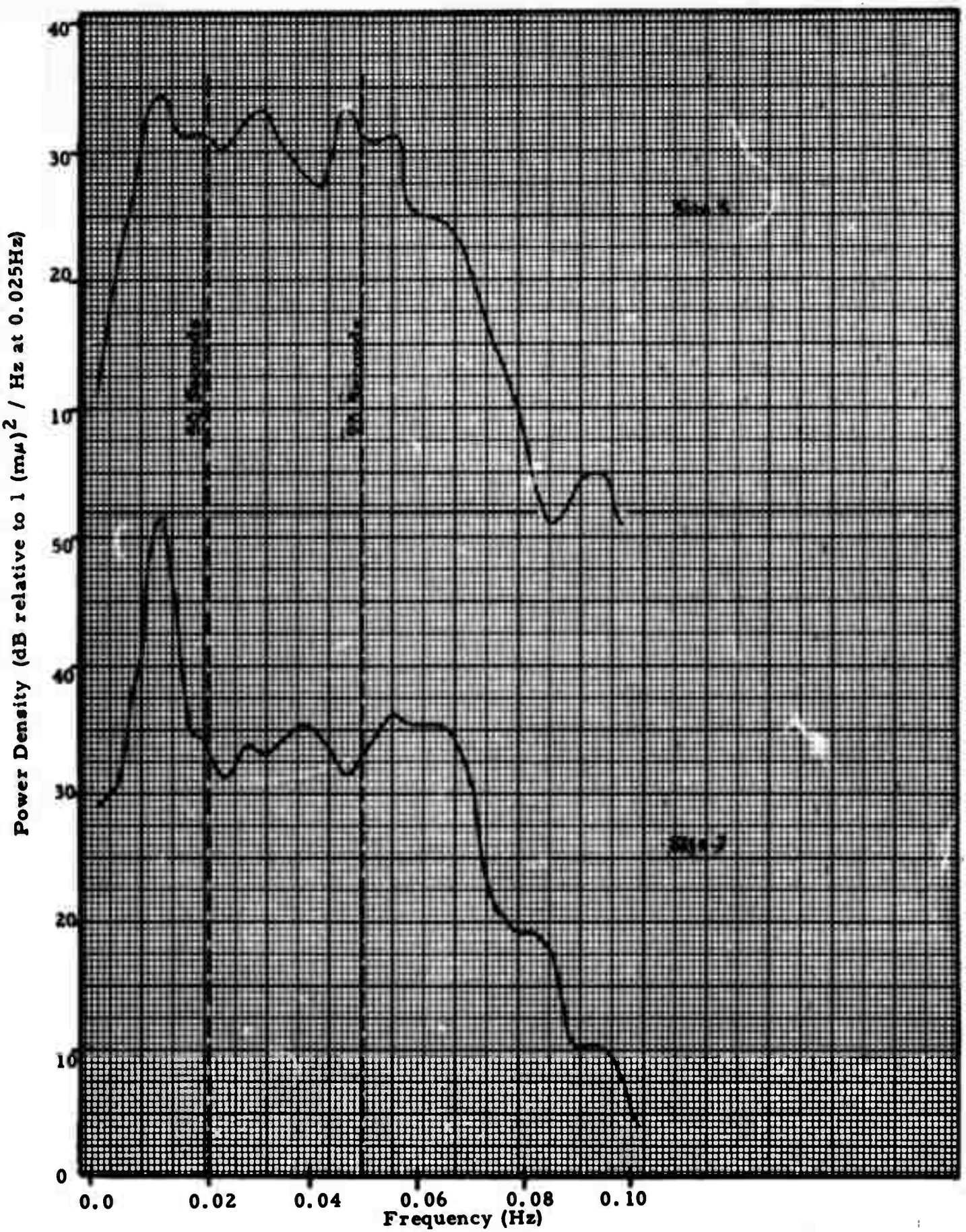


FIGURE VI-2
NOISE POWER DENSITY SPECTRA
(vertical components only) 1/26/71, 10:00

## 2. Time Variability

The time variability of the noise field at each of the sites, over the January 24, 1971 to February 6, 1971 time period was studied by computing the RMS level in the 20-40 second band. After computation, the levels were corrected to absolute ground motion using the Lamont calibration data. It should be noted that the 20-40 second responses are reasonably close between the vertical and horizontal components for sites 1, 2, and 5. However, the vertical response for site 3 (Alaska) is about twice that of the North-South component. Thus a direct component comparison can be made for all sites except 3 (Note: no responses were available for site 7). RMS calculations are shown in Figure VI-3. From this figure the following conclusions have been made:

Site 1 - very little can be said due to the limited amount of data but the East-West horizontal appears to be the noisiest. The difference between the maximum and minimum component RMS levels are: vertical = 4.4, North-South = 2.7, and East-West= 6.0

Site 2 - an increasing trend in noise level with time is seen for all three components. The difference between the maximum and minimum component RMS levels are: vertical= 4.5, North-South= 6.6, and East-West= 3.8. Also, the two horizontal components are much higher than the vertical component. This difference also is visible in the spectra and is most pronounced at the longer periods.

Site 3 - as opposed to site 2, the vertical component is the noisiest for site 3. A possible explanation for the noisier vertical is that the conversion to ground motion was done using the calibration information at 40 seconds. Because of the difference in amplitude response between the vertical and horizontals for Alaska,

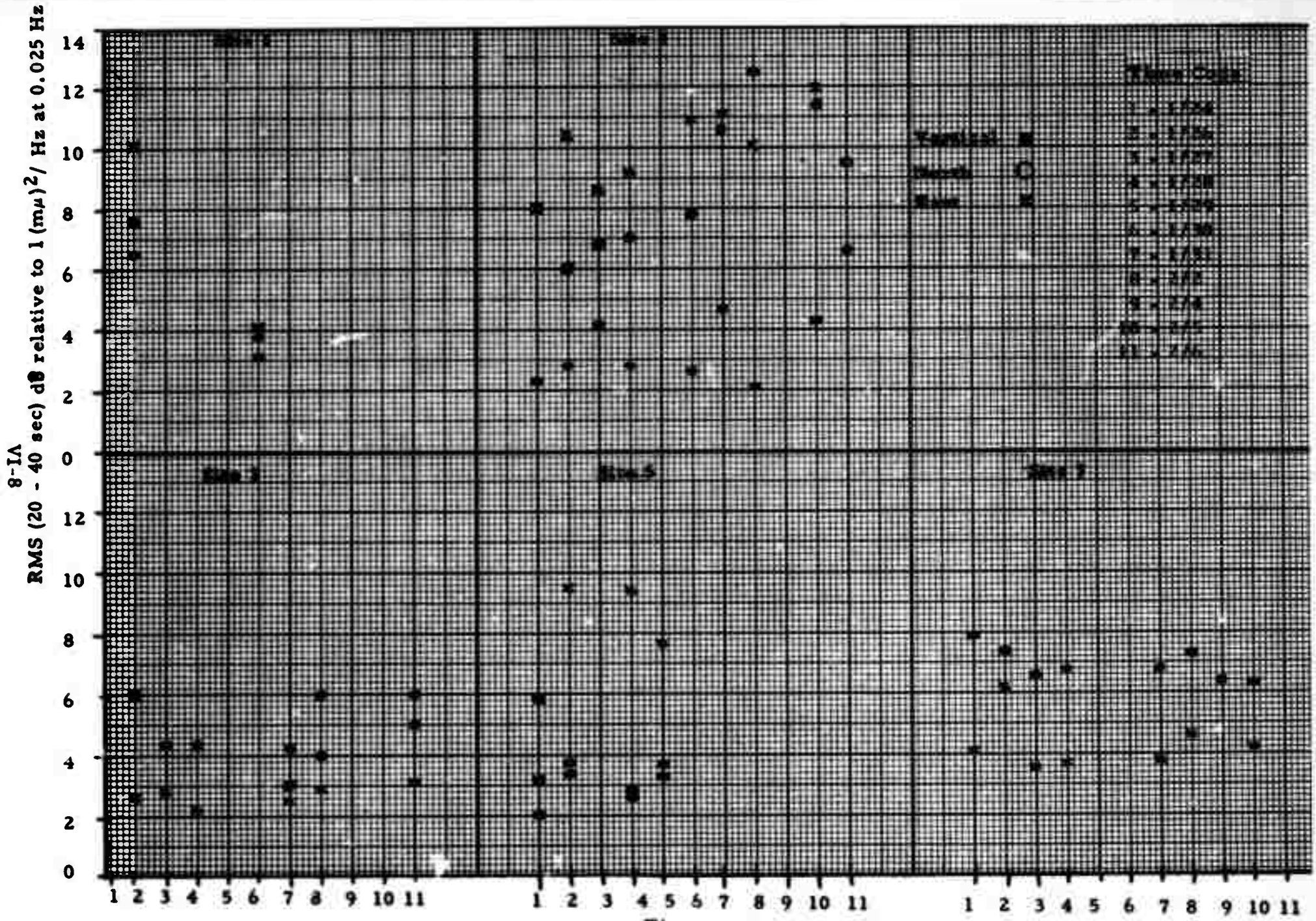


**FIGURE VI-3**
**NOISE RMS LEVELS**

the vertical would have a higher RMS level than the horizontals in the 20-40 second band if the absolute noise spectra were identical. However, the noise levels do tend to remain fairly constant through most of the time period (Note: the North-South component was not operating correctly for samples 1-4). The difference between the maximum and minimum component RMS levels are: vertical= 1.7, North-South= 3.1, and East-West= 0.9

Site 5 - the noise level for the vertical and North-South components remain fairly level. However, observing the large difference between the two horizontal RMS levels, it appears that the amplitude scale factor may be suspect for the East-West component. The difference between the maximum and minimum component RMS levels are: vertical= 1.2, North-South= 2.5, and East-West= 3.7.

Site 7 - the vertical and East-West components appear to remain fairly constant throughout the time period. The difference between the maximum and minimum component RMS levels are: vertical= 1.6, and East-West= 0.9. Again the vertical component is noisier. Since no frequency response was available for site 7, we could not check to see if the noisier vertical component was due to the instruments responses as for site 3. (Note - the North-South component appeared to have been replaced with another vertical instrument, since it had essentially the same data points as the vertical component.

In general, except for site 2, the noise field RMS levels tend to remain fairly constant during the time period. Also the RMS levels for sites 2 and 3 vertical components, site 5 vertical and North-South components, and site 7 East-West

component all are similar. Further, it appears that the horizontal components are noisier than the vertical components. The LPE RMS levels are the same order of magnitude as those observed at ALPA and NORSAR.

C. Signal Processing

1. Event Detection

This section discusses the detection capability of the five stations and of the network for the 19 events (Table VI-3) recorded during the period January 24, 1971 to February 6, 1971. This event ensemble includes all reported events from the Asian continent during the time period (both USCGS and LASA), except those which were buried in large interfering events at all sites. Also, any site which was down or the data was bad is not included in the detection or not-detected plots. All results are from the vertical component unless otherwise specified, and all results are based on data which has only been bandpass filtered (no matched filtering or 2-component processing was performed).

Figure VI-4 is a detection plot for $m_b$ versus delta - the following observations are made from this figure:

Site 1 - all events with $m_b > 4.8$ were detected

Site 2 - all events with delta $< 50^\circ$ and all events with $m_b > 4.8$ were detected

Site 3 - all events with delta $< 60^\circ$ and all events with $m_b > 4.8$ were detected

Site 5 - all events with delta $< 80^\circ$ and all events with $m_b > 4.8$ were detected

Site 7 - all events with delta $< 75^\circ$ and all events with $m_b > 4.8$ were detected

The dotted lines on Figure VI-4 separate the plots into zones of complete detection (for the data sample analyzed) and partial detection; note that several events with $m_b < 4.8$ and delta $> 70^\circ$ were detected at sites 3, 5, and 7.

TABLE VI-3

LPE EVENTS

1/24/71 TO 2/6/71

( All detections on LR vertical unless otherwise specified)

| EVENT DESCRIPTION | | | | | SITES | | | | | | | | | |
|---|---|---|---|---|---|---|---|---|---|---|---|---|---|---|
| Source Date | Source Time | Latitude Deg. | Longitude Deg. | $m_b$ | Australia | | Thailand | | Alaska | | Israel | | Ogdensburg, NJ | |
| | | | | | Δ | Det. | Δ | Det. | Δ | Det. | Δ | Det. | Δ | Det. |
| 1/24 | 13:21:16 | 49.2N | 156.3E | 4.9 | 70 | ✓ | 55 | ✓ | — | | 86 | ✓ | 79 | ✓ |
| 1/24 | 13:28:44 | 49.2N | 156.1E | 5.0 | 70 | ✓ | 55 | ✓ | — | | 86 | ✓ | 79 | ✓ |
| 1/24 | 13:47:36 | 49.1N | 156.3E | 4.6 | 70 | B | 55 | B | — | | 86 | ✓ | 79 | ✓ |
| 1/25 | 00:11:43 | 53.9N | 162.4E | 4.7 | 75 | B | 59 | B | — | | 85 | B | 73 | B |
| 1/25 | 18:42:25 | 49.2N | 156.4E | 4.7 | 70 | B | 55 | B | — | | 86 | B | 79 | B |
| 1/26 | 22:48:31 | 43.8N | 39.2E | 4.8 | 116 | N | 56 | N | 71 | N | 15 | ✓ | 76 | N |
| 1/27 | 19:57:55 | 47.9N | 154.0E | 4.8 | 68 | N | 53 | N | 35 | ✓ | 86 | N | 81 | N |
| 1/28 | 15:51:07 | 35.0N | 47.0E | 4.6 | 109 | N | 49 | ✓ | 79 | N | 12 | ✓ | 87 | ✓ |
| 1/29 | 21:23:43 | 55.7N | 163.5E | 4.6 | — | | — | | 25 | ✓ | 84 | ✓(LQ) | 71 | ✓(LQ) |
| 1/30 | 20:15:41 | 30.5N | 79.1E | 4.6 | — | | 22 | ✓ | 78 | ✓ | — | | 104 | ✓ |
| 2/1 | 01:12:27 | 37.2N | 30.2E | 4.5 | — | | 62 | ✓ | 78 | ✓ | — | | 76 | ✓ |
| 2/1 | 14:21:43 | 42.3N | 85.3E | 4.8 | 84 | D | 26 (S wave LR doubtful) | | 65 | N | — | | 95 | N |
| 2/2 | 07:59:57 | 23.8N | 91.8E | 5.4 | — | | 8 | ✓ | 80 | ✓ | — | | 114 | ✓ |
| 2/4 | 02:54:05 | 53.0N | 162.8E | 4.6 | 75 | N | 59 | N | 27 | B | — | | 74 | B |
| 2/4 | 05:27:46 | 44.0N | 45.9E | 4.5 (LASA) | 111 | N | 51 | N | 71 | N | — | | — | |
| 2/5 | 09:09:58 | 25.2N | 99.4E | 5.3 | 64 | ✓ | 6 | ✓ | 76 | ✓ | — | | 114 | ✓ |
| 2/6 | 00:58:42 | 44.9N | 148.0E | 4.3 (LASA) | — | | 48 | ✓ | 40 | ✓ | — | | — | |
| 2/6 | 16:34:11 | 38.1N | 73.3E | 4.5 | — | | 30 | D | 72 | ✓ | — | | — | |
| 2/6 | 22:12:45 | 36.0N | 69.9E | 5.0 | — | | 31 | ✓ | 75 | ✓ | — | | — | |

DETECTION CODE

✓ = Detection  B = Buried Event

N = No "  D = Bad Data

— = No Data

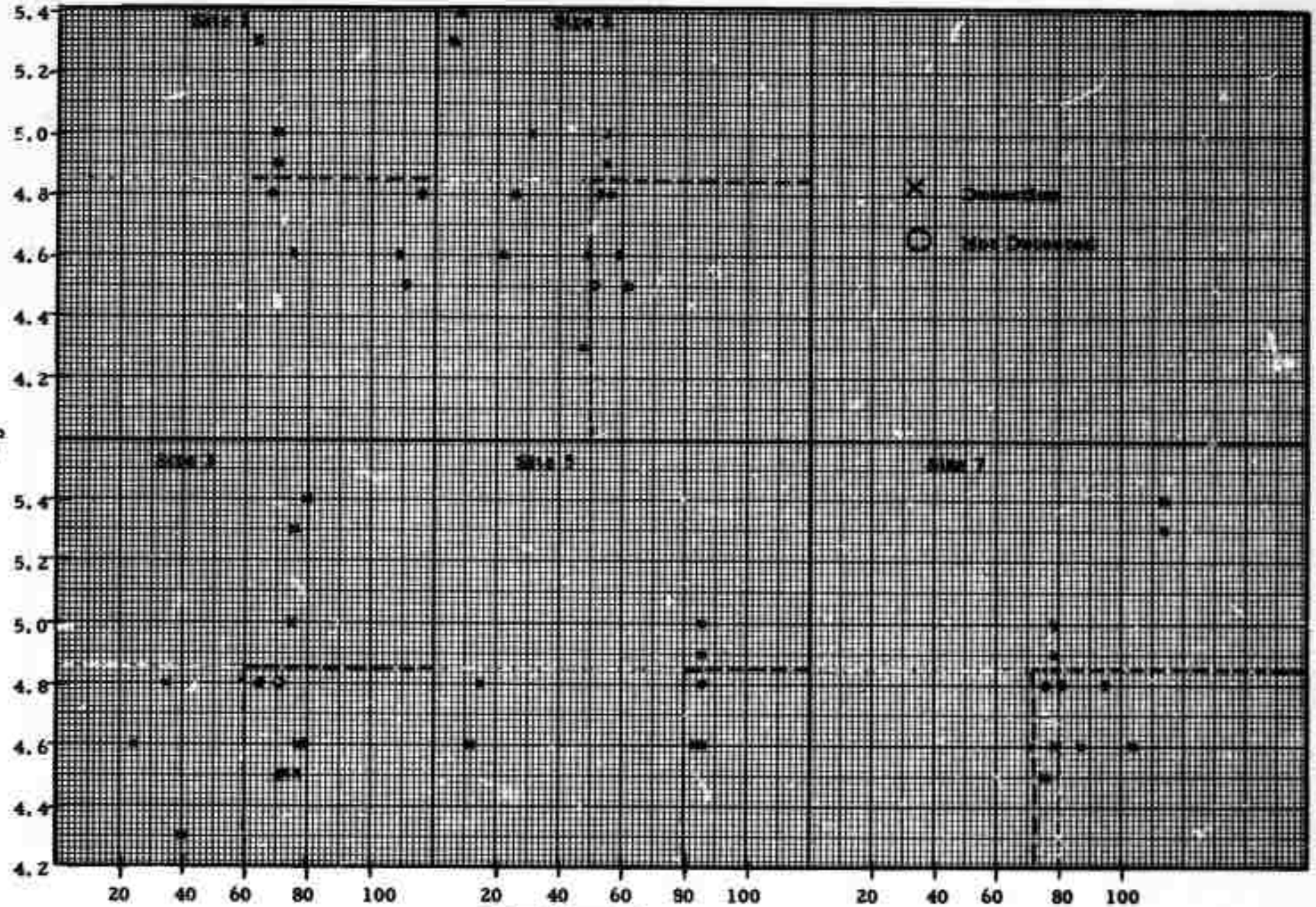


FIGURE VI-4

EVENT DETECTION ($m_b$ vs. Delta) FOR INDIVIDUAL SITES

The data of Figure VI-4 were replotted with $M_s$ vs delta, where $M_s$ was calculated by:

$$M_S = \log \frac{A}{T} + .92 + \log \Delta \qquad \Delta < 25^o$$

$$M_S = \log \frac{A}{T} + 1.66 \log \Delta \qquad \Delta \geq 25^o \qquad \text{(Evernden, 1971)}$$

Note that two of the events, $m_b = 4.5$ and 4.6, were not detected at any stations and thus no $M_s$ value for then could be calculated. For a given event $M_s$ was averaged over all detecting stations and this average value was used to plot $M_s$ versus delta for each site. The $M_s$ versus delta plot for the individual sites is shown in Figure VI-5. Observations from this figure are:

- The events tend to separate into detected and not-detected classes, although there is some overlap (sites 2, 3, and 7).
- There is a tendency for the " detection threshold" to increase with distance (as would be expected) but the sparse data are not sufficient to specify a "detection threshold line"
- It appears that at $60^o$ most stations have a detection threshold between $M_s = 3.0$ and $M_s = 3.4$. The small range of this detection level among stations agrees with the small variance in RMS noise levels for their vertical components. (Note: there is not enough noise data to make this comparison for site 1).

Figure VI-6 is a composite of Figures VI-4 and VI-5. The top half of the figure shows $m_b$ versus delta for all stations. As in Figure VI-4, scattering is evident, however, for the events analyzed the following observations can be made for the five-station network:

- all events with $m_b > 4.8$ were detected at all operating stations
- all events were detected at all operating stations having delta $< 50^o$

The bottom half of the figure is a plot of delta versus $M_s$ for all stations. This plot shows the expected increase in detection threshold with dististance. The broken lines show the probable range in detection threshold as a function of distance, because all stations appear to have similar sensitivity this curve is a very crude estimate of an individual station detection capability.

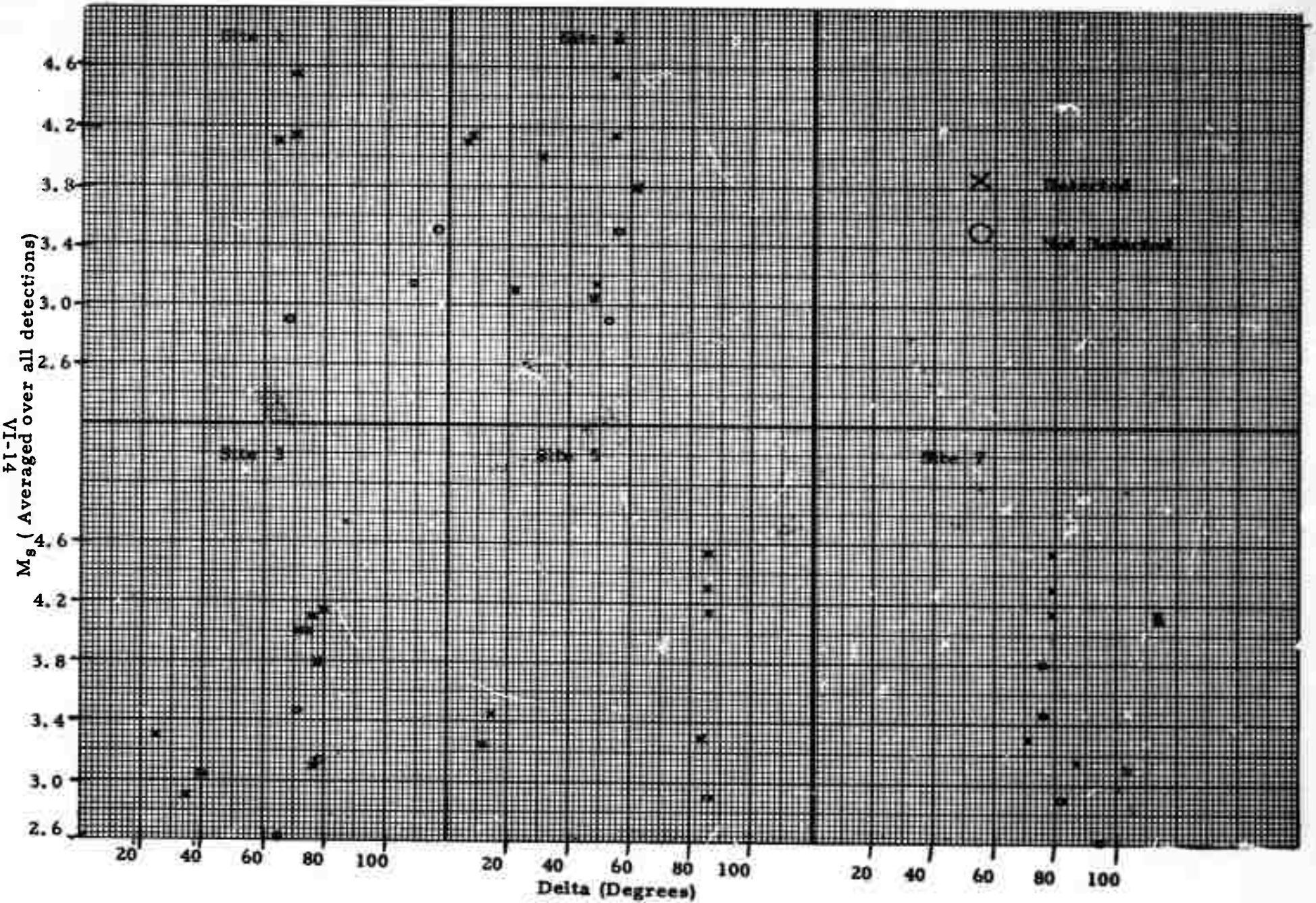


FIGURE VI-5

EVENT DETECTION ($M_s$ vs. Delta) FOR INDIVIDUAL SITES

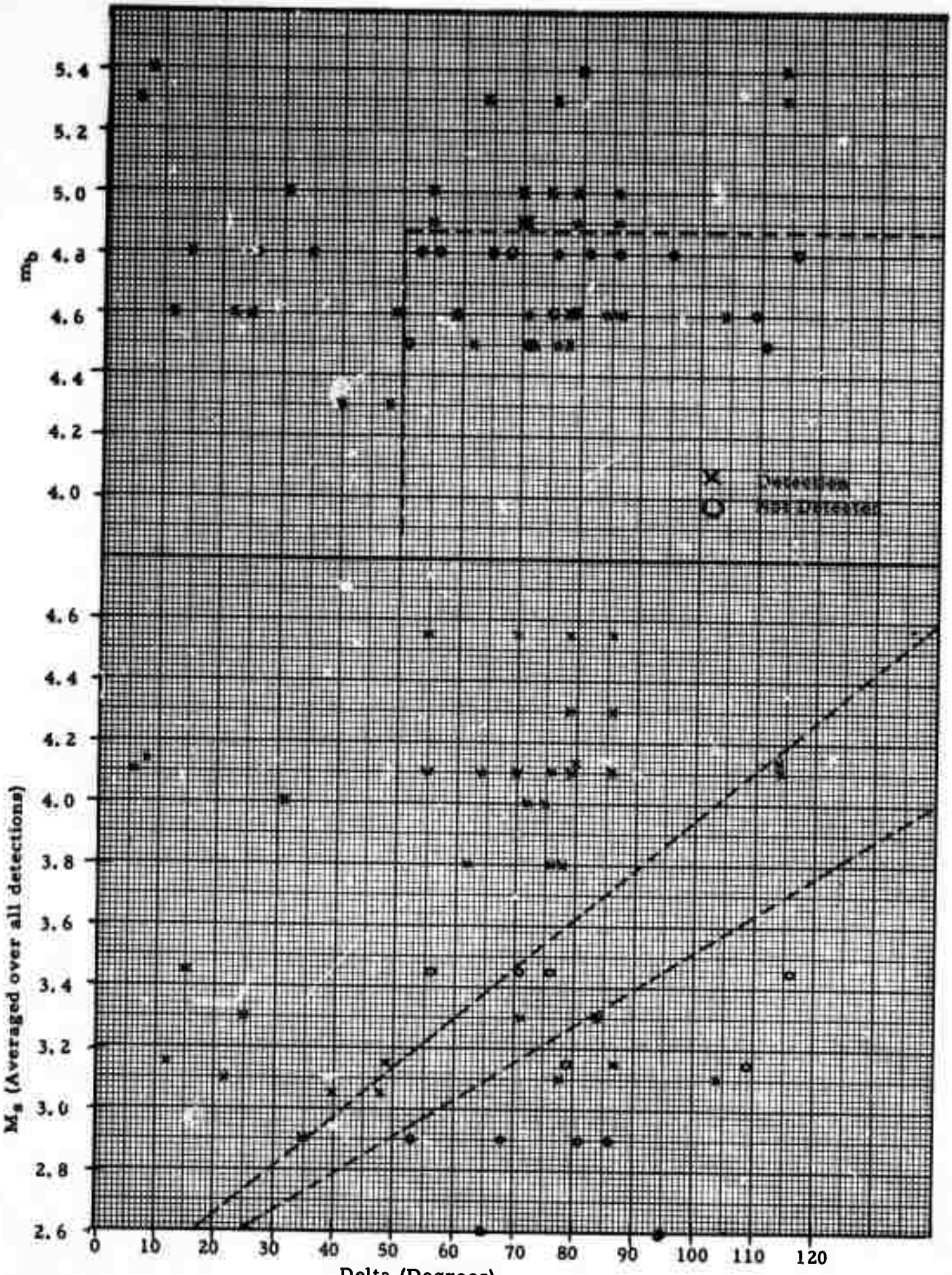


FIGURE VI-6

NETWORK DETECTION

It is important to remember that these graphs are not intended to present a definitive network or individual station detection threshold, but are presented only to show the results obtained from analysis of a very limited number of events.

2. Behavior of Standard Discriminant

To study the behavior of a standard discriminant for the LPE network, an $M_s$ versus $m_b$ plot for the individual sites was prepared. (Figure VI-7). This figure shows a large amount of scattering in the $M_s$ values for any given event (as much as 1.2 units for the 5.3 $m_b$ event). Note that each event is coded with the same symbol for all sites. The Gutenburg $M_s$-$m_b$ relationship for earthquakes (Richter, 1958) fits the observed data reasonably well. All of the events are separated from the broken line, which was obtained from Capon's data (1967) for a series of Asian explosions.

Figure VI-8 is a repeat of Figure VI-7 using an average $M_s$ for each event. It should be noted that the $M_s$= 2.6 event was calculated from one site and that is was calculated from a probable LR phase; an S phase from the event was clearly detectable on the LP vertical component, while the LR wave was not larger than the largest noise peaks. However, again we see a fairly good fit to the Gutenburg curve and generally good separation from Capon's curve.

D. Future Plans

In the near future we expect to begin receiving data from all five of the stations in Table VI-1 plus the station in Spain. When these data are received we plan to enter a routine processing mode (20-40 events per month). However, until such data are available, we plan to begin processing the data for August,1971 (after the station modifications) for Australia, Alaska, and Ogdensburg. Current data at SAAC for the period is for days 220-236 (August 8-24).

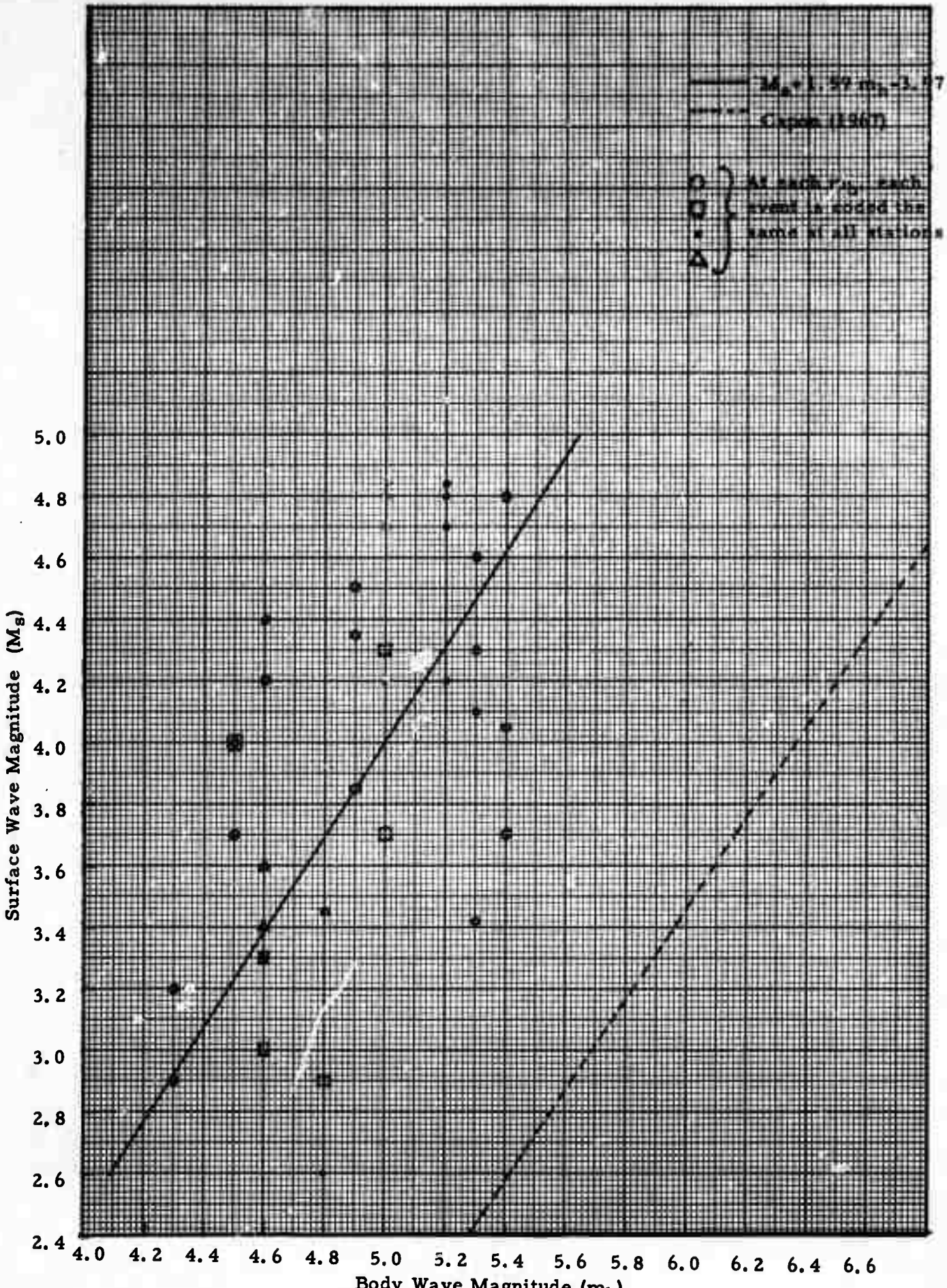


FIGURE VI-7
$M_s$ vs. $m_b$ FOR ALL SITES